ENVIRONMENTAL RESEARCH INSTITUTE OF MICHIGAN
FORMERLY WILLOW RUN LABORATORIES, THE UNIVERSITY OF MICHIGAN
P. O. BOX 618 • ANN ARBOR • MICHIGAN • 48107
PHONE (313) 483-0500

INFRARED AND OPTICS DIVISION
TECHNOLOGY APPLICATIONS

19 September 1973

193300-24-L

National Aeronautics and Space Administration
Goddard Space Flight Center
Greenbelt Road
Greenbelt, Maryland 20771

Attention: Mr. E. F. Szajna, Code 430

Contract: NAS5-21783

Subject: Sixth Bimonthly (Type I) Report for Period Covering 1 July 1973 - 31 August 1973

Dear Sir:

The enclosed material comprises the sixth (6th) bimonthly technical report for contract NAS5-21783, which describes the progress for the ten tasks of the Environmental Research Institute of Michigan program for the subject period. It is noted that this report covers the 13th and 14th months of the contractual period, which is the seventh bimonthly period. The required financial reports 533M and 533Q are submitted separately from ERIM's accounting department. The work on this contract is performed in the Radar and Optics Division (Task IV only) under the direction of Dr. L. J. Porcello and in the Infrared and Optics Division (for the other nine tasks) directed by Mr. R. R. Legault.

Principal investigators for each task are listed in each subsection of this report for the ten tasks. A summary listing of the tasks by number, principal investigator and short title is provided as an attachment to this letter. Titles of papers produced during this reporting period and their authors also are listed as an attachment to this letter.

The status, principal activities and accomplishments of the various tasks for this reporting period are noted here in summary form.

A new technique for obtaining water depth information from ERTS MSS data has been developed, which will be tested soon on ERTS data (Task I). A 14 color land use map for the Yellowstone Park area is being prepared, which will be followed by a quantitative assessment of the map's accuracy (Task II). Data processing which had been long delayed for Task III is now under way with the receipt of the CCT's, which will

ENVIRONMENTAL RESEARCH INSTITUTE OF MICHIGAN
FORMERLY WILLOW RUN LABORATORIES, THE UNIVERSITY OF MICHIGAN
P. O. BOX 618 • ANN ARBOR • MICHIGAN • 48107
PHONE (313) 483-0500

permit submittal of a Data Analysis Plan soon. Task IV is shifting from emphasis on analysis of fresh-water ice formations to assessing the impact of lake shore erosion in selected Great Lakes areas utilizing both ERTS MSS data and aircraft collected radar data. ERTS imagery indicates good data should have been obtained for the Oakland County, Michigan, area so that processing of tapes when received can be made for recreational and open space studies for the area (Task V - at this writing, tapes have just been received). The Lake Ontario Basin study for the IFYGL is making rapid progress in (1) defining the actual area of the Lake Ontario Basin and (2) analog processing of the MSS data for land use recognition for the basin area (Task VI). Weather conditions during July and August prevented obtaining desired ERTS underflight data with the ERIM aircraft, but calibration measurements were made on the Bendix RPMI and a paper was completed on the integration of ERTS data with earth based coordinate systems (Task VII). The water quality monitoring program has continued analysis of ERTS frame data for Lake Erie and the New York Bight; in these analyses an ERTS data problem has been encountered by Task VIII, which is similar to that encountered by Task VII earlier (and reported in the second Type II report under Task VII). Initial efforts to detect an oil slick in the Oakland (California) Inner Harbor area using ERTS digital data have not been successful; another attempt will be made on the Monongahela oil spill of early June (Task IX). An automatic recognition map derived from MSS channel ratio techniques for a portion of the Wind River Range area in Wyoming is being studied for iron bearing rock identifications by comparison with recently collected ground truth and geologic maps for the area (Task X).

Reports prepared by the individual investigators follow in order by task number.

Respectfully submitted,

F. J. Thomson

Frederick J. Thomson
Research Engineer

Approved by: Paul R. Lea

Richard R. Legault
Director, Infrared and Optics Division

FJT/RRL/njm

Attachments:
List of Tasks
List of current papers from the Tasks
Type I reports for each of the ten tasks.

ERTS PROGRAM SUMMARY

Under Contract NAS5-21783

TASK	PRINCIPAL INVESTIGATOR	MMC #	UN	SHORT TITLE
I	Polcyn	063	200	Water Depth Measurement
II	Thomson	077	621	Yellowstone Park Data
III	Thomson	137	636	Atmospheric Effects (Colorado)
IV	Bryan	072	201	Lake Ice Surveillance
V	Sattinger	086	225	Recreational Land Use
VI	Polcyn	114	635	IFYGL (Lake Ontario)
VII	Malila Nalepka	136	612 178	Image Enhancement
VIII	Wezernak	081	625	Water Quality Monitoring
IX	Horvath	079	606	Oil Pollution Detection
X	Vincent	075	422	Mapping Iron Compounds

LIST OF PAPERS FROM THE TASKS FOR REPORTING PERIOD

TASK	TITLE
IV	(1) Fresh-Water Ice Interpretation from ERTS Imagery by M. L. Bryan
	(2) Multifrequency Simultaneous Radar Imagery by M. L. Bryan
VII	(1) Correlation of ERTS Data and Earth Coordinate Systems by W. Malila, R. Hieber and A. McCleer
X	(1) Spectral Ratio Imaging Methods for Geological Remote Sensing from Aircraft and Satellites by R. K. Vincent (in process).

Sixth Type I Progress Report - 1 July 1973 - 31 August 1973
Task I - Water Depth Measurement - 1388
F. C. Polcyn, UN 200, MMC 063

The current water depth program, which is based on a ratio technique, gives reliable results up to a depth of about 3 meters when used with ERTS data. For greater depths the MSS channel 5 signal (.60-.70 μm) is so small that the ratio of the signals in channels 4 and 5 is not a meaningful index of the water depth.

In processing the Bahama Bank data, water depths up to 9 meters were mapped using a two-step process. Depths of shallow areas were obtained from the depth program, and these results were correlated with the channel 4 signal (.50-.60 μm). The final depth map was then obtained from the channel 4 signal, calibrated by the results of the depth program.

To eliminate this two-step process a new technique is being explored for extracting water depth information from multispectral signals collected over water. The technique is based on the fact that there is a linear correlation between the logarithms of the bottom-reflected signals in two or more spectral channels over water of variable depth. This correlation may be expressed as follows:

$$\log V_2 = k + \frac{\alpha_2}{\alpha_1} \log V_1 \qquad (1)$$

where V_1 = signal in channel 1

V_2 = signal in channel 2

α_1 = water attenuation coefficient in channel 1

α_2 = water attenuation coefficient in channel 2

k = a constant depending on the bottom reflectance, scanner sensitivity, and irradiance at the water surface.

Because of noise, the actual data points will be scattered about the line represented by equation (1). In order to classify these points according to water depth, decision boundaries are constructed perpendicular to this line. The equation for the decision boundary corresponding to a depth z_i is

$$\log V_2 = k_i - \frac{\alpha_1}{\alpha_2} \log V_1 \qquad (2)$$

Thus, points falling between the decision boundary for z_1 and the decision boundary for z_2 are classified as having a depth between z_1 and z_2.

This depth criterion is equivalent to the following formula, which is valid for any number, N, of signal channels:

$$z = z_o - \frac{1}{c} \sum_{i=1}^{N} \alpha_i \log V_i \qquad (3)$$

The constants z_o and c can be determined using equations (3) and (4).

$$V_i = V_{oi} \exp \{-\alpha_i (\sec \theta + \sec \phi)\, z\} \qquad (4)$$

where θ = scan angle

ϕ = solar zenith angle, and

V_{oi} = the signal received over zero water depth.

The results are:

$$c = (\sec \theta + \sec \phi) \sum_{i=1}^{N} \alpha_i^2 \qquad (5)$$

$$z_o = \frac{1}{c} \sum_{i=1}^{N} \alpha_i \log V_{oi} \qquad (6)$$

Alternately, z_o may be determined if the signal $(V_{ref})_i$ at a known depth z_{ref} is known:

$$z_o = z_{ref} + \frac{1}{c} \sum_{i=1} \alpha_i \log (V_{ref})_i \qquad (7)$$

A program implementing this technique is being written, and will be tested with suitable ERTS data when such data are received.

The high gain tape made during a test run over the Atlantic coastline has not yet been received.

Sixth Type 1 Progress Report - 1 July 1973 - 31 August 1973
Task II - Yellowstone National Park Data - 1398
F. J. Thomson, UN 621, MMC 077

Dr. Smedes and Mr. Root (a graduate student assisting Dr. Smedes) reported to ERIM by phone their qualitative accuracy estimates of the 13 category terrain feature recognition map at the end of July. Their report, in essence, stated the majority of terrain feature categories were quite accurately identified, commission errors between categories were low, and production of a color-coded concise display of the classification results was thus warranted.

This final 14 color map (13 categories of terrain features plus an unclassified category) will be generated by the Mead Corporation (Dayton, Ohio) on their concise display device. This apparatus requires 9 track digital tapes as input; consequently, conversion of ERIM's 7 track output tapes to a compatible 9 track format is necessary.

This is currently underway using a reformatting routine originally written by ERIM programmers to accomplish this same task for ERTS data of the "San Francisco Frame." We expect to ship the reformatted classification output tapes to Mead Corporation the first week of September.

Upon our receipt of the concise display product we will photograph it and send copies to Dr. Smedes to assist him in his analysis program.

Several high quality frames of MSS data of the Yellowstone-Grand Teton area have been received during the recent months. The relative advance and retreat of winter snow cover is striking. Of additional interest, the absence of snow accumulation around Yellowstone's well known hydrogeothermal areas. Progress in timber harvesting along Yellowstone's western boundary is also apparent.

Plans are now being made for writing the final report, which will commence upon the conclusion of Dr. Smedes' quantitative accuracy analysis of the final map.

Sixth Type I Progress Report - 1 July 1973 - 31 August 1973
Task III - Atmospheric Effects in ERTS-1 Data - 1410
F. J. Thomson, UN 636, MMC 137

This reporting period saw the initiation of processing activity connected with the recognition mapping phase of the task. CCT's were finally received for frames 1009-17075 (1 August 1973), 1028-17135 (20 August 1973), and 1208-17145 (16 February 1973). Discussion with the co-investigator (Dr. Smedes) has resulted in the selection of the 20 August 1972 frame for recognition mapping of the test site. Data of that frame have been graymapped (Band 5) and will be shipped to the co-investigator for placement of training set locations. Recognition mapping will proceed when training set locations are returned.

The investigation of atmospheric effects on ERTS data will begin during the next reporting period. Preliminary plans call for using water bodies and snow surfaces on the 20 August 1972 and 16 February 1973 data, respectively as standards for assessing the effects of varying base altitude on atmospheric transmission. Further development of processing plans is contingent upon closer inspection of the data and discussions with the co-investigator. From these activities, we expect that a Data Analysis Plan will be defined and submitted by 15 October.

Atmospheric measurements collected by Hulstrom of Martin-Marietta, coincident with ERTS overpasses of 16 February and 21 June 1973, have been received and are being studied. These measurements are intended for correlation with the processing results of the ERTS data, however, some concern exists as to their total adequacy for such a correlation. In order to provide for a complete documentation of weather conditions at the time of ERTS overpasses, weather records have been ordered from several surrounding reporting stations for specific dates of interest.

The program for the next reporting period will comprise the following activities: 1) the recognition map of the test site will be completed for the 20 August 1972 data, 2) a Data Analysis Plan will be finalized and submitted, 3) digital processing to determine the effects of varying base altitude on atmospheric transmission will begin, 4) weather records ordered from the National Weather Records Center will be studied and correlated with atmospheric measurements made by Hulstrom, and 5) additional ERTS frames will be screened and appropriate CCT's ordered.

Sixth Type I Progress Report - 1 July 1973 - 31 August 1973
Task IV - Lake Ice Surveillance - 1406
M. Leonard Bryan, UN 201, MMC 072

1. Ice Surveillance

The ground truth data which were secured (using the BENDIX RPMI instrument) during March 1973 have been studied with respect to the ERTS-1 imagery. Interpretation techniques, ground truth (spectral) and visual information from the Ice Information Center of the U.S. Coast Guard, are presented in a separate report, "Fresh-Water Ice Interpretation from ERTS Imagery", by M.L. Bryan, U201, ERIM (this report is being submitted to NTIS). It is noted that the interpretations made have required little in terms of sophisticated instrumentation which argues strongly for the use of ERTS-1 data by researchers and scientists who have limited time, and lack the funds and instrumentation required for detailed machine analysis. An example of such a need is the 'real time' use of these data for ship navigators in the Great Lakes during the critical periods of the navigation season. It is obvious that more detailed and precise analyses can be conducted with automatic data processing techniques. However, this precision is possibly not needed for some navigation problems and, considering the time delay for processing, assuming the timely receipt of ERTS-1 data, would not be warranted when information concerning ice, or similar ephemeral earth surface features, is considered.

2. Change in Data Analysis Plan

The following letter was received by Dr. Leonard J. Porcello from R.D. Phillips (Contracting Officer, NASA, GSFC)on 13 August 1973.

Environmental Research Institute of Michigan
Attn: Leonard J. Porcello
P.O. Box 618
Ann Arbor, Michigan 48107

Subject: ERTS-1 Contract NAS5-21783, MMC#72, Data Analysis Plan Approval

A review of the status of the subject investigation has been made. It has been decided that, owing to the poor quality of both environmental conditions and ERTS imagery received by you, that the work relating to the application of remote sensing to the surveillance of lake ice be suspended. Instead, you are hereby authorized to enter Phase III activity and to perform a study concerning the application of ERTS imagery to the Great Lakes shore flooding problems. In particular, this study shall include the investigation of the geographic processes of areas located in Monroe, Macomb and Wayne Counties, Michigan, which include the shoreline along Lakes Erie and St. Clair.

This authorization does not include or imply any approval of increases in costs.

R. D. Phillips
Contracting Officer

3. Some of the work discussed in the contracting officer's letter has been initiated, as was indicated in the second Type II report. The work conducted to this time has been only a first look analysis of the radar data and a preliminary report of this work is presented in "Multifrequency Simultaneous Radar Imagery" by M. L. Bryan, U201, ERIM (which is being submitted separately to NTIS).

4. Planned Activities for the Next Reporting Period

   a. Complete SLAR data processing,
   b. Expand the type of visual interpretation of SLAR data following the format indicated in the report noted in 1 above,
   c. Comparison of the ERTS-1 data with the SLAR data and completion of a report covering the results, as indicated in the letter, see 2, above.

5. Discussion of Results

   a. The separate report (noted in 1, above) presents the results of qualitative and visual analysis of several ERTS-1 frames. More detailed ground truth would place us in the position of being able to present further analyses and also would permit the initial development of an identification key for fresh-water ice features as shown on ERTS-1 imagery. The report on ice interpretation presents a scheme and the methodology needed for preparation of such a key.
   b. The report (noted in 3, above) presents a discussion of the interpretation of simultaneous side-looking Synthetic Aperture Radar imagery. It will be recalled that initially the project was to compare ERTS-1 imagery with simultaneous SLAR imagery. However, as indicated in the letter quoted above, the program has been altered insofar as the geographical location described by the data is concerned. Hence, a statement concerning the first aspects of efforts based on the changed work statement is included in the radar imagery report (see 3, above).
   c. There are no cost-benefit comments at this time.

6. ERTS Image Descriptor Forms

   One copy enclosed as Appendix A.

7. Data Request Forms Submitted to GSFC/NDPF

   One was submitted on 29 August 1973. Copy is enclosed as Appendix B.

ERIM
FORMERLY WILLOW RUN LABORATORIES, THE UNIVERSITY OF MICHIGAN

ERTS(I) TYPE I REPORT

05 Sept. 1973

ERTS IMAGE DESCRIPTOR FORM

APPENDIX A

M. L. Bryan, #U201

Environmental Research Institute of Michigan
P. O. Box 618
Ann Arbor, Michigan 48107

ERTS IMAGE DESCRIPTOR FORM

(See Instructions on Back)

NDPF USE ONLY
D
N
ID

DATE 05SEP73

PRINCIPAL INVESTIGATOR M.LEONARD BRYAN

GSFC #U201

ORGANIZATION ENVIRONMENTAL RESEARCH INSTITUTE OF MICHIGAN

PRODUCT ID (INCLUDE BAND AND PRODUCT)	FREQUENTLY USED DESCRIPTORS*			DESCRIPTORS
1197-16095X	Lake ice	snow		contrails
1249-15582X	lake ice	snow	Pleistocene Beaches	

*FOR DESCRIPTORS WHICH WILL OCCUR FREQUENTLY, WRITE THE DESCRIPTOR TERMS IN THESE COLUMN HEADING SPACES NOW AND USE A CHECK (✓) MARK IN THE APPROPRIATE PRODUCT ID LINES. (FOR OTHER DESCRIPTORS, WRITE THE TERM UNDER THE DESCRIPTORS COLUMN).

MAIL TO ERTS USER SERVICES
CODE 563
BLDG 23 ROOM E413
NASA GSFC
GREENBELT, MD. 20771
301-982-5406

GSFC 37-2 (7/72)

NDPF USE ONLY

D
N
ID
AA
TM

DATA REQUEST FORM

1. DATE 29AUG73

2. USER ID U201

4. SHIP TO:

ADDRESS Dr. M.Leonard Bryan ☐ NEW

Environmental Res. Inst. Michigan

P.O. BOX 618

ANN ARBOR, MI. 48103

5. TELEPHONE NO. (313)483-0500 X-204 ☐ NEW

6. CATALOGUES DESIRED

STANDARD ☐ U.S. ☐ NON-U.S.

DCS ☐

MICROFILM ☐ U.S. ☐ NON-U.S.

APPROVAL TECHNICAL MONITOR _____

ADDDHHMMSS OBSERVATION IDENTIFIER	C CENTER POINT COORDINATES	B SENSOR BAND	P PRODUCT TYPE	F PRODUCT FORMAT	T TICK MARKS	NN NUMBER OF COPIES	A AREA
1197-16095	N44-37 W087-43	M		P		2	U
1197-16095	N44-37 W087-43	M		T		1	U
1249-15582	N46-02 W084-30	M		P		2	U
1249-15582	N47-02 W084-30	M		T		1	U
1197-16095	N44-37 W087-43	7	B	T		1	U
1249-15582	N46-02 W084-30	7	B	T		1	U

TABLE OF CONTENTS

TABLE OF CONTENTS (CON'T)

INTRODUCTION

Two recent publications (McClain, 1973 and Wendler, 1973) have added to the literature dealing with the utility of the ESSA series of satellites for making observations of sea ice in the Arctic. These articles describe the composite minimum brightness (CMB) technique used for the study of ice types, their spatial distributions, and the identification of ice and cloud covered areas. Although much work has been published concerning satellite data for the study of snow and other glaciological features, little work has been presented on the utility of these data for the study of the types, distribution, and movement of fresh-water lake ice.

Data from a new high resolution satellite is now available to the general public. This satellite, the National Aeronautics and Space Administration (NASA) Earth Resources Technology Satellite (ERTS(I)), operates in four spectral bands from an orbit at 915 km and yields data with a ground resolution of approximately 91 m. A single image covers a rectangular area approximately 185 km on a side, with each scene being retaken (within 37 km) once every 18 days. Because the satellite orbit is sun synchronous, each scene is re-viewed at approximately the same time each 18th day, and consequently, major problems resulting from variable solar lighting conditions are minimized. More complete information is available in: A) ERTS Data User's Handbook[a] (description of the satellite system, including the orbital characteristics and processing at the National Data Processing Facility (NDPF) ; B) ROUSE AND SITER (1973) (brief summaries of the ERTS(I) work being conducted under the

auspices of NASA); and C) NASA Earth Resources Survey Program weekly abstracts [b] (a continuing update of the progress being made by the ERTS(I) projects).

ERTS(I) STUDIES:

Several papers concerning the interpretation of ERTS(I) imagery with respect to snow and sea ice are available. BARNES and BOWLEY (1973a), in discussing the interpretation of ERTS(I) data for mapping of snow-line elevation in western United States, determined that ERTS(I) Band 5 was the single most useful band. (See Table 1 for spectral range of individual bands). Band 4 also showed a significant difference between snow cover and snow free terrain, while Band 7 was determined to be least useful for this differentiation. Of particular interest is the comment that "Although a thorough investigation of the multispectral characteristics of snow has not yet been undertaken, examination of data from the Arctic has revealed that the multispectral approach can provide information on glacial conditions that cannot be ascertained from observations in a single spectral band."

MEIER (1973) speaks to a similar set of problems in identification of snow-lines and glacial features in high mountains of western United States and Alaska. He notes that mapping of snowlines from ERTS(I) imagery is highly dependent on cloud cover and vegetation, and to a lesser degree, on solar angle, terrain roughness and slope, radiometric fidelity and spectral information. No data are given regarding the last of these parameters, although one would suppose that Bands 4 and 6 were considered to give the best information for this work as these were the

bands used in the illustrations. Comments concerning glacial interpretation do, incidentally, support the observations made by BARNES and BOWLEY (1973a) quoted above.

BARNES and BOWLEY (1973b) report using ERTS(I) imagery for the identification of sea ice in the Arctic. Their conclusions are that Bands 4 and 7 are the best two bands for identification of ice features, while Bands 4 and 5 are preferred for identifying ice boundaries. By using several bands in concert their results are more reproducible. Unfortunately, no imagery or attempt at quantification of the spectral responses were included in the report, and the nature of the ground truth is often in doubt.

RADIOMETRIC GROUND TRUTH:

Many radiometric data have been collected over ice and snow surfaces for various types of studies, including remote sensing (e.g., HORVATH and BROWN, (1971)). It is necessary that a proper ground truth operation be conducted in support of remote sensing and that the field data be collected for the same bands of the electromagnetic spectrum as those in which the sensor is operating. To aid in the collection of the necessary radiometric ground truth data in conjunction with the ERTS(I) satellite, three instruments are available: (1) The Bendix Radiant Power Measuring Instrument (RPMI)[(c)] ; (2) the EXOTECH MODEL 100[(d)] ; (3) the Gamma Scientific Monitor[(e)]. These instruments can be used for obtaining incident radiation (using a 180° hemispherical field of view) and for measuring scene reflectance. For the latter measurements, the RPMI has a solid angle field of view (FOV) of 6° whereas the EXOTECH has a FOV of 15°.

The radiometric response is an integration of the measurement over the entire scene viewed or in the case of the satellite for the data (resolution) cell. Some problems can thus arise, especially where a very detailed reading of the ground may represent only a small portion of the ERTS(I) resolution cell. Consequently, it is necessary not only to measure large areas, but also to obtain numerous measurements over similar surfaces if it is hoped that the ground truth reading may be able to be adequately related to the ERTS(I) images for interpretative purposes.

Another major problem for ERTS(I) image interpretation (which is likely to arise), given the existence of the target reflection data, is the calculation of the atmospheric attenuation scattering of the energy between the ground and the satellite sensors. ROGERS and PEACOCK (1973) have worked on this problem and present the theory for calculating atmospheric parameters (beam transmittance, path radiance), determining target reflectance and then employing these parameters for translating the ERTS(I) data into the desired target reflectance characteristics. Our concern, in the present paper, is to present several modified target reflectance curves for snow and fresh water ice features in the ERTS(I) spectral bands, which upon application of the correction techniques may possibly allow accurate machine and human interpretation of the ERTS(I) data.

This type of radiometric ground truth is important for snow and ice studies because:

a) The shape, size and location of the subject is, especially in the case of pack ice, constantly changing and consequently

cannot always be accurately applied to interpretation over a time series of satellite images;

b) Especially in the spring and fall in higher latitudes and throughout the winter in mid-latitudes, the temperature of the surface material is fluctuating around the freezing point. Consequently, the surface is alternating from wet to dry - the rate of this fluctuation being dependent on weather and meteorological conditions prevailing at the time.

DATA:

Radiometric ground truth data for six types of ice and snow surfaces were collected during the 1972-1973 winter season at two sites (Douglas Lake, Emmett County and Whitmore Lake, Washtenaw County) in Michigan (Fig. 1). The six surfaces studied were: a) drained and refrozen slush; b) new snow; c) dry white ice; d) slush and water mixture; e) close pack (ice concentration .7 - .9); and f) open pack (concentration .4 - .6). For each site, four readings were taken; global irradiance; sky irradiance; direct beam irradiance and reflected radiance. Only the first and last of these are considered in this paper. All data were collected between 1000 and 1400 local sun time on days when the sky was clear and essentially cloud free. No data were taken when clouds obscured direct sun radiation to the observation site. All data were collected using the Bendix RPMI instrument which is thoroughly described by ROGERS and PEACOCK (1973).

Figure 2 illustrates the variations in site reflectance, as a percentage (X 100) of global irradiance, for the six surfaces. These data were collected using the Bendix 6° FOV, with the instrument oriented

normal to the surface and at an elevation of 1.0 meters. Essentially, then, this figure is a statement of the albedo in the four ERTS(I) bands for these surfaces. For each surface type, 8 to 10 sets of readings were made. Both the average and one standard deviation of the readings are plotted (Fig. 2) for each surface and for each ERTS(I) band. In this figure G is the outgoing radiation (using 6° FOV); O is incoming radiation (180° hemisphere).

ERTS(I) data, in the form of imagery (Figs. 3 and 6) and included as examples of anticipated application of the radiometric ground truth data of the type presented in Fig. 2. The two study sites are Whitefish Bay, Michigan (29 March 73, ERTS(I) identification number 1249-155582) and Green Bay, Wisconsin (05 Feb. 1973, ERTS(I) identification number 1197-16095). Locations for these two sites are included in Fig. 1.

ANALYSIS OF DATA:

1. Whitefish Bay, Michigan

If we assume that the six classifications of ice (Fig. 2) adequately cover the types to be expected in the ERTS(I) imagery and that all ice in the ERTS(I) scenes are liable for classification into one of these six types, we can then, based partially upon the radiometric data, develop an identification map of the lake ice.

Whitefish Bay, on the Michigan/Ontario border (Figs. 3, 4 & 5), has several features which are immediately apparent. Other than the jet contrail, trending SE-NW across the center of the bay, atmospheric interference with the ERTS(I) scene is of apparently minimal importance

for this qualitative study. Shorelines and islands are easily distinguished, as are the Pleistocene beaches on Whitefish Point.

A.) Open Water: the areas of open water are identified as those having, in all four images, very low reflectance, and, from the Band 7 image, essentially no reflectance at all. Although not included in Fig. 2, to use only Band 7 for open water recognition would be to possibly include both types of pack ice and also the slush/water classification. On Band 7 open water could not be confused with white ice, snow or drained slush (Fig. 2). Likewise, leads and other large openings in the ice are clearly identified using the same bands as for open water.

B.) Drained Slush:

Some ice in Tahquamenon Bay is best classified as 'drained slush'. We note from Fig. 1 that there is a slight rise in the reflectance between Bands 4 and 6 and then a rather large (relative to the other bands) drop in reflectance in Band 7. This type of surface is slush which has apparently refrozen slowly during a period when the free water has been draining out - thus it is highly porous, has a relatively low density and has a texture similar to that of a frozen sponge. Consequently, it has a rough surface (at least at these wavelengths) and, because of its porous nature, scatters a great amount of light incident upon it. This ice therefore implies a given height above the water level, or, given a lower elevation, a relatively calm sea during periods of the draining. It also implies the existence of meteorological conditions being very close to the freezing point - sufficient to allow draining prior to

refreezing, but not to allow extensive melting of the entire ice parcel.

C.) Snow: Snow has a lower albedo but, contrary to the other surfaces studied, this albedo is approximately constant in all four ERTS(I) bands. Several areas of snow are seen in the northern portion of the ice cover in Whitefish Bay. These areas, if properly identified, indicate ice which has a slight snow cover but of some indeterminable thickness and which is essentially free of free water. It is thus reasonable to state that the ice underlying the snow is solid, free of cracks, and fissures and also that the weather has been sufficiently cold to prevent melting of this snow.

D.) White Ice: White ice with a dry surface apparently covers a very large portion of the entire imaged area. Figure 2 indicates that although there is a drop in the albedo of this ice type with increasing wavelength, this drop is small and the reflection in Band 7 is still quite sufficient to be detected by the ERTS(I) system. Consequently, the white ice should be easily differentiated from the surface types previously mentioned because of the changes in the reflectance curves and from those of lower reflectance (Fig. 2) due to the reflectance in the 0.8 - 1.1 μm band. White ice is essentially frozen slush and is, in several respects, a variation of the 'drained slush' discussed above. In the white ice case, however, the water has been trapped and has been refrozen in place so that the density is much higher (approximately 0.75 to 0.90) and the porosity is reduced considerably. This ice type does not generally imply any given thickness and is one which, from the navigational point of view, probably should be avoided.

E.) Slush and Water/Light and Heavy Pack: These three types have the common feature of being poor reflectors in the ERTS(I) Band 7. Reflectance at the short wavelengths (Band 4) portion of the spectrum is also decreasing as the amount of water visible to the sensors increases. The reflectance is decreased and generally, in addition to the decrease in reflectance, there is an increase in the standard deviation. The latter is especially prominent in the case of the light pack. Some reflectance will be possible for all surfaces studied depending upon the amount of open water. The total area of ice needed for reflectance has not been determined and would, in any case, be partially a function of the sensitivity of the sensor employed.

In the Whitefish Bay area, several areas are identified. The area in the general vicinity of Waiska Bay is classed as being predominantly slush and water. This decision is based upon reflectance but is also contingent upon the smooth and unbroken texture seen on the ice. One small area (probably dry white ice) extends across the center of this patch in a southwest-northeast direction.

Finally, areas of pack ice are seen to the north and northwest of the bay. These areas have degrading reflectances with increasing wavelengths and are, in many cases, nearly imperceptible on the Band 7 image. No attempt is made to distinguish the heavy and light packs from one another.

No simultaneous ground truth data are available for ERTS(I) scene, but the ice reconnaissance data for the previous day have been located. These data (Fig. 5) are based on visual aircraft reconnaissance.

The two data are not really comparable because they are dealing with two different classifications of ice. (In fact, this is also true of the ERTS(I) reflectance data). They also deal with two distinct time periods. However, we note that the main body of ice in Whitefish Bay is classed as rafted (to heights of 3-15 feet) in areas having coverage of 4-9 tenths ice. The more protected bays (Tahquamenon and Goulais) are, based on these visual observations, free of ridged ice. These visual data also suggest that transportation through the main body of ice in Whitefish Bay would be quite treacherous. However, given the lateness of the season and the amount of open water, ship passage should be safe within several days to several weeks (i.e., the first part of April) during this particular year. In fact, the first ship did clear the locks at Saulte St. Marie just to the east of the study area, on (29 March 1973, SS John Munson), the day these ERTS(I) data were collected

2. Green Bay, Wisconsin

A second area of interest, Green Bay, Wisconsin, was also considered (Fig. 1). The data are approximately six weeks earlier (05 Feb. 73) and, consequently, the ice coverage is more continuous and, in general, the areas of different spectral reflectances are more distinct and sharply identified.

Figure 7 is the interpretation of ice for Green Bay. The ice reflectance from Band 7 strongly suggests that a very large portion of the study area is covered with free water, but the high reflectance of some of the same areas in the other three bands indicates that many of these 'free water' areas are not open ice free water but have underlying

ice features. The rationale for the interpretation of Figure 6 is as described for the Whitefish Bay, Michigan case and based partially on the reflectance curves presented in Fig. 2. Figure 7 presents the interpretation of ERTS(I) imagery, and Figure 8 presents the visual aircraft observations.

DISCUSSION:

The extraction of ice information from aerial photography is a well developed and useful aspect of air photo interpretation and photogrammetry (e.g. MARSHALL, 1966). As with other aspects of photo interpretation, the addition of imagery obtained with multiband cameras and the further sophistication of the spectral concept to the multispectral scanners (as used on ERTS(I)) has added a new dimension into the science and also, in many respects, to the level of information and detail which can be extracted. Numerous machine techniques are available for interpretation and for presentation of the data in a visual format. These are generally based upon the spectral recognition of various surfaces which are to be studied. Spectral responses, in the very straight forward manner and as used herein, are one method of approaching the subject. A more sophisticated approach requires computer hardware with a large storage capability and the decision-making software to compare the responses for each data cell in the study area and then to compare various combinations of the spectral responses for each band and for each data cell. A discussion of these methods is quite beyond the purposes of the paper.

Of pertinence in this present data is, however, the fact that ice data from fresh-water areas are available via the ERTS(I) satellite and,

more importantly, it appears as if useful information can easily be extracted from these data. The necessary basic inputs, the spectral reflectance curves, for both generic and genetic ice types are necessary if the type of work which is being discussed is to become operational. Spectral curves and a complete spectral library of ice types, possibly collected with both ground and aircraft based sensors, and for the same spectral bands as used on the ERTS(I) satellite should be the next logical step for the progression of this type of work. Then machine processing could be conducted with accuracy and validity.

A comment concerning the term 'operational' is needed. Although it is technically possible to produce automatic recognition maps based upon spectral curves from the ERTS(I) data, these data would probably be useful only for scientific and historical, as opposed to operational (near real-time), functions. This is because the ERTS(I) satellite passes over a given area only once each 18 days, its data collection ability may be curtailed by cloud cover (e.g., Fig. 6) and finally because the delay between the time of satellite pass and data collection and its ultimate delivery to the investigator is presently in the neighborhood of 4-6 weeks. This latter problem may, however, be corrected in the future. For more isolated areas or where the immediacy of such information is pertinent, it may be compensated for by the acquisition of a data read-out apparatus operated by the investigators. This possibility is, however, very expensive and would be beyond the financial capabilities of most non-government organizations.

CONCLUSIONS:

The spectral reflections of several types of ice and in the same bands as the NASA ERTS(I) satellite have been presented and used, in a very basic way, to demonstrate their ability for interpretation of fresh-water ice conditions. The study situations are taken from the Great Lakes of North America. Snow covered ice, white ice, slush and water, two types of pack ice drained slush and open water are identified. However, the purpose of the paper is to present the nature of the problem of ice identification from a high altitude, medium resolution (approximately 91 m) satellite system rather than to present definite interpretation techniques. The problem is one which needs considerable additional study. Although all ERTS(I) bands are considered to be of importance in interpretation of the data, some bands, and combinations of bands, are of greater importance than others - which ones these are is dependent upon the nature of the problem to be investigated. At present, this type of work has limited utility for real time operational work (e.g., planning immediate ship movements) while the utility for scientific studies of ice distribution, movement and type identification, is much greater.

TABLE 1

ERTS-MSS Spectral Response

BAND	NDPF Band Code	Wavelength (Micrometers)
1	4	.5 - .6
2	5	.6 - .7
3	6	.7 - .8
4	7	.8 - 1.1

FOOTNOTES

(a) Data Users Handbook: Prepared for NASA, Goddard Space Flight Center, Greenbelt, 20771 by: General Electric, Space Division. Valley Forge Space Center. PO Box 8555. Philadelphia Pa., USA. 19101. Purchase Price $10.00

(b) NASA Earth Resources Survey Program Weekly Abstracts
Available from: U.S. Dept. Commerce. National Technical Information Service, 5285 Port Royal Road Springfield, VA. 22151

(c) Bendix Aerospace Systems Division, 3300 Plymouth Road, Ann Arbor, Michigan 48107

(d) EXOTECH, Inc. 1200 Quince Orchard Blvd., Gaithersburg, Md. 20760

(e) Gamma Scientific, Inc., 3777 Ruffin Road, San Diego, Calif. 92123

REFERENCES

1. Armstrong, T., B. Roberts, C. Swinthinbank, 1969. Illustrated Glossary of Snow and Ice. Cambridge, Scott Polar Research Institute. 60pp.

2. Barnes, J. C. and C. J. Bowley, 1973a. "Use of ERTS Data for Mapping Snow Cover in the Western United States". Symposium on Significant Results Obtained from the Earth Resources Technology Satellite - Vol. 1. Washington, D. C. NASA, SP-327, pp. 855-862.

3. Barnes, J. C., and C. J. Bowley, 1973b "Use of ERTS Data for Mapping Arctic Sea Ice". Symposium on Significant Results Obtained from the Earth Resources Technology Satellite - Vol. 1. Washington, D. C. NASA. SP-327. pp. 1377-1384.

4. Horvath, R. and W. L. Brown, 197]. Multispectral Radiative Characteristics of Arctic Sea Ice and Tundra. Ann Arbor, Mich. Institute Sci. & Technology. Willow Run Labs. Report 27980-2-F July ix + 63 pp.
(prepared for the Arctic Institute of North America, Agreement ONR-426)

5. McClain, E. P., 1973 "Quantitative Use of Satellite Vidicon Data for Delimiting Sea Ice Conditions". Arctic, V 26, No. 1, Mar. pp. 44-57.

6. Marshall, E. W., 1966. Air Photo Interpretations of Great Lake, Ice Features. Ann Arbor, Michigan. University of Michigan, Institute of Science & Technology, Great Lakes Research, Special Report No. 25, ix + 92 pp.

7. Meier, M. F. 1973, "Evaluation of ERTS Imagery for Mapping and Detection of Changes of Snowcover on Land and on Glaciers." Symposium on Significant Results Obtained from the Earth Resources Technology Satellite, Vol. 1, Washington, D. C., HASA SP-327, pp. 863-875.

8. Rogers, R. H. and K. Peacock, 1973. "A Technique for Correcting ERTS Data for Solar and Atmospheric Effects". Symposium on Significant Results Obtained from the Earth Resources Technology Satellite - Vol. 1., Washington, D. C., NASA SP-327, pp. 1115-1122.

9. Rouse, J. W., Jr. and S. Siter. "ERTS Experiments". IEEE Transactions on Geoscience Electronics, V. GE-11, No. 1 Jan. pp. 3-77.

10. Wendler, G., 1973, "Sea Ice Observations by Means of Satellites." Journal of Geophysical Research, V. 78., No. 9, Mar 20. pp. 1427-144

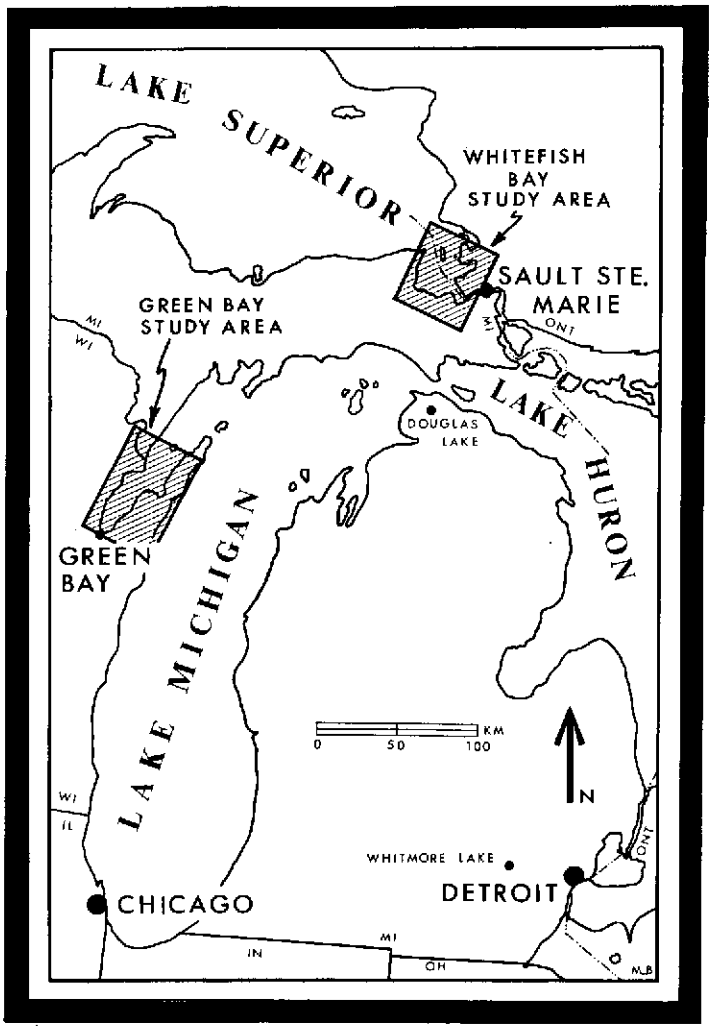

FIGURE 1. LOCATION OF STUDY AREAS

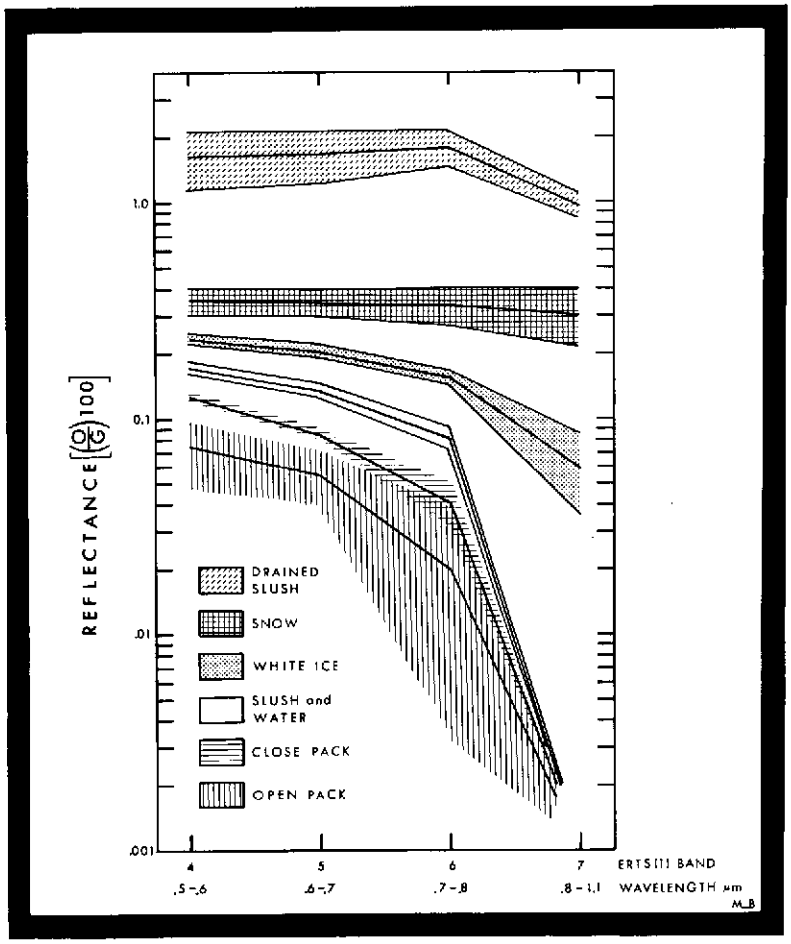

FIGURE 2. SPECTRAL RESPONSE FROM ICE AND SNOW SURFACES.
(See Text for Discussion.)

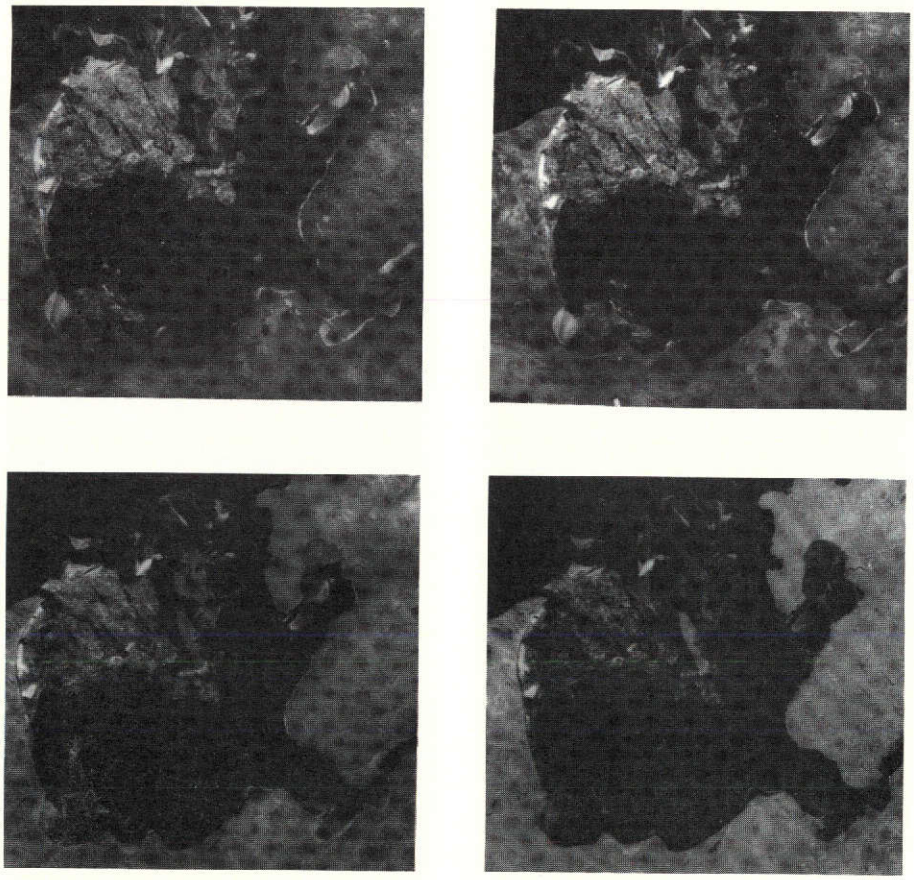

FIGURE 3. ERTS(I) IMAGERY. Whitefish Bay, MI. 29MAR73. Scene 1249-15582. (UL Band 4; UR Band 5; LL Band 6; LR Band 7.)

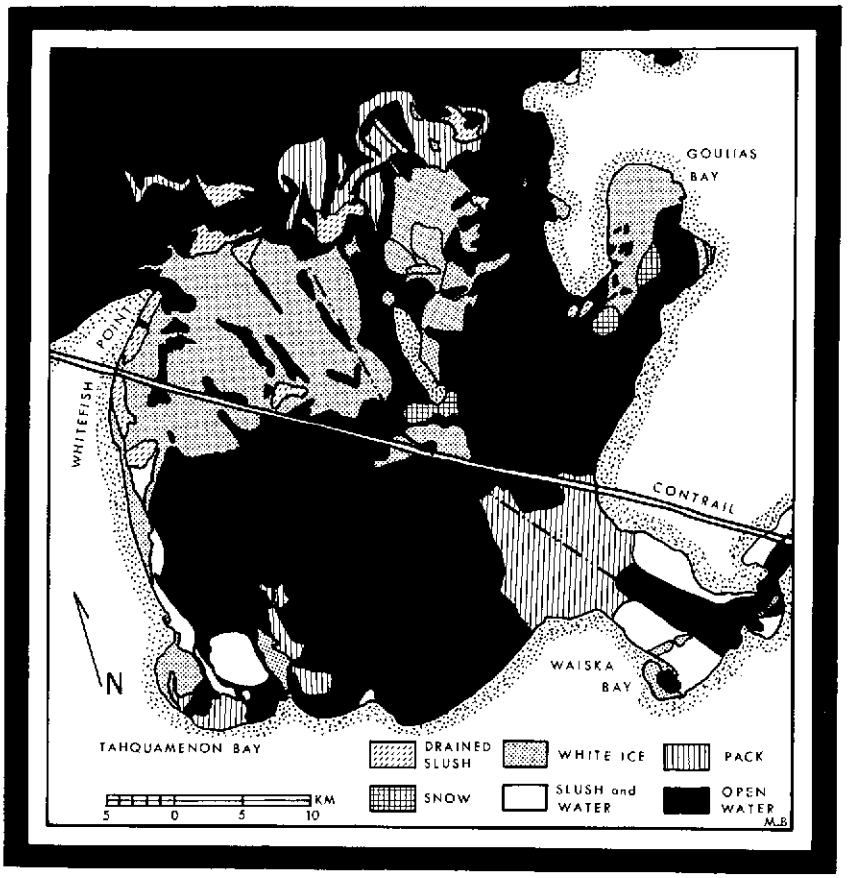

FIGURE 4. INTERPRETATION OF ERTS(I) IMAGERY FOR WHITEFISH BAY, MI. Scene: 1249-155582.

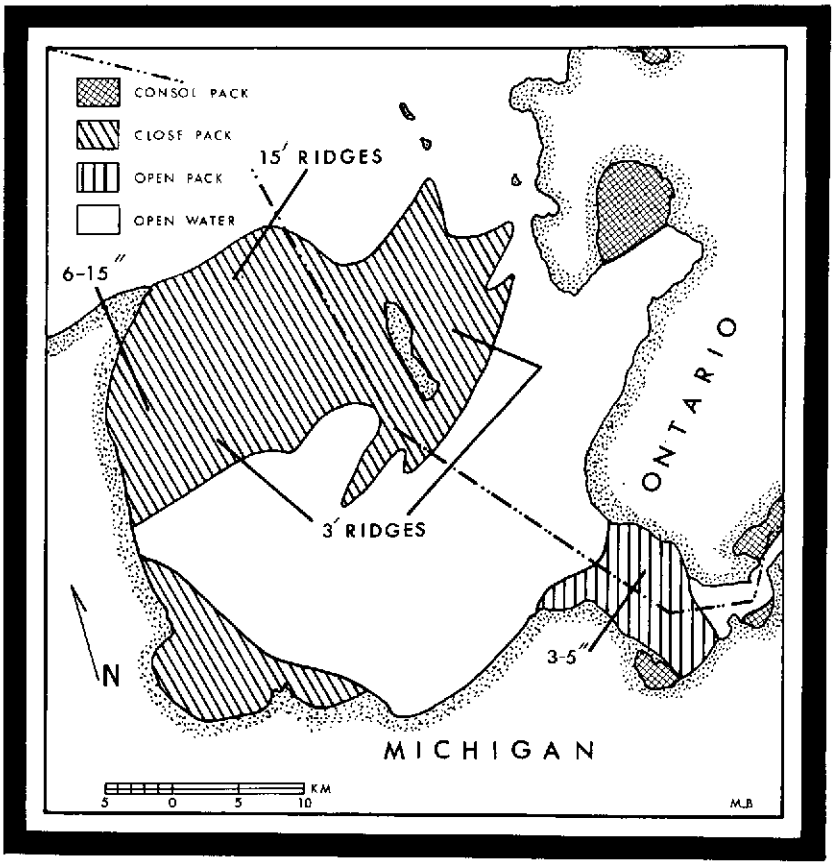

FIGURE 5. ICE ON WHITEFISH BAY, MI. 28MAR73. (SOURCE: U.S. Lake Survey, Detroit, MI.)

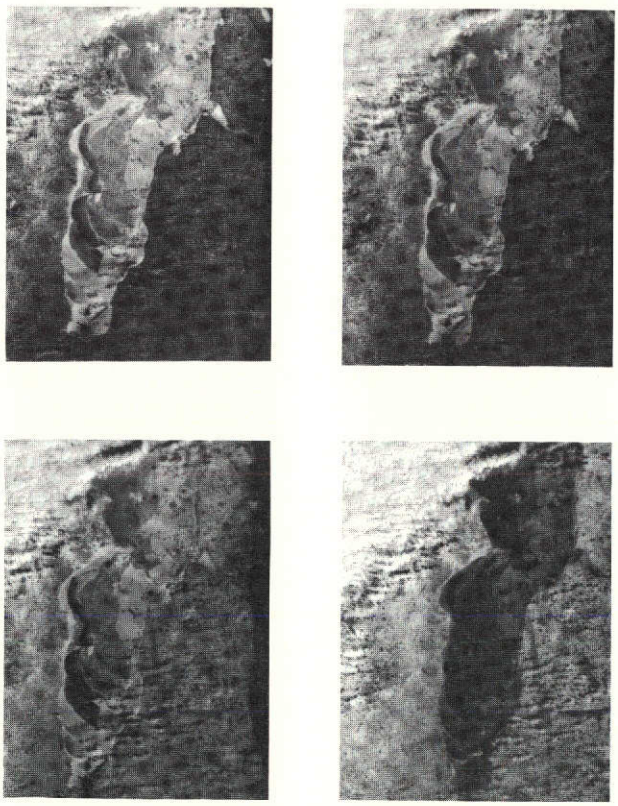

FIGURE 6. ERTS(I) IMAGERY. Green Bay, WI. 05FEB73. Scene: 1197-16095. (UL Band 4; UR Band 5; LL Band 6; LR Band 7.)

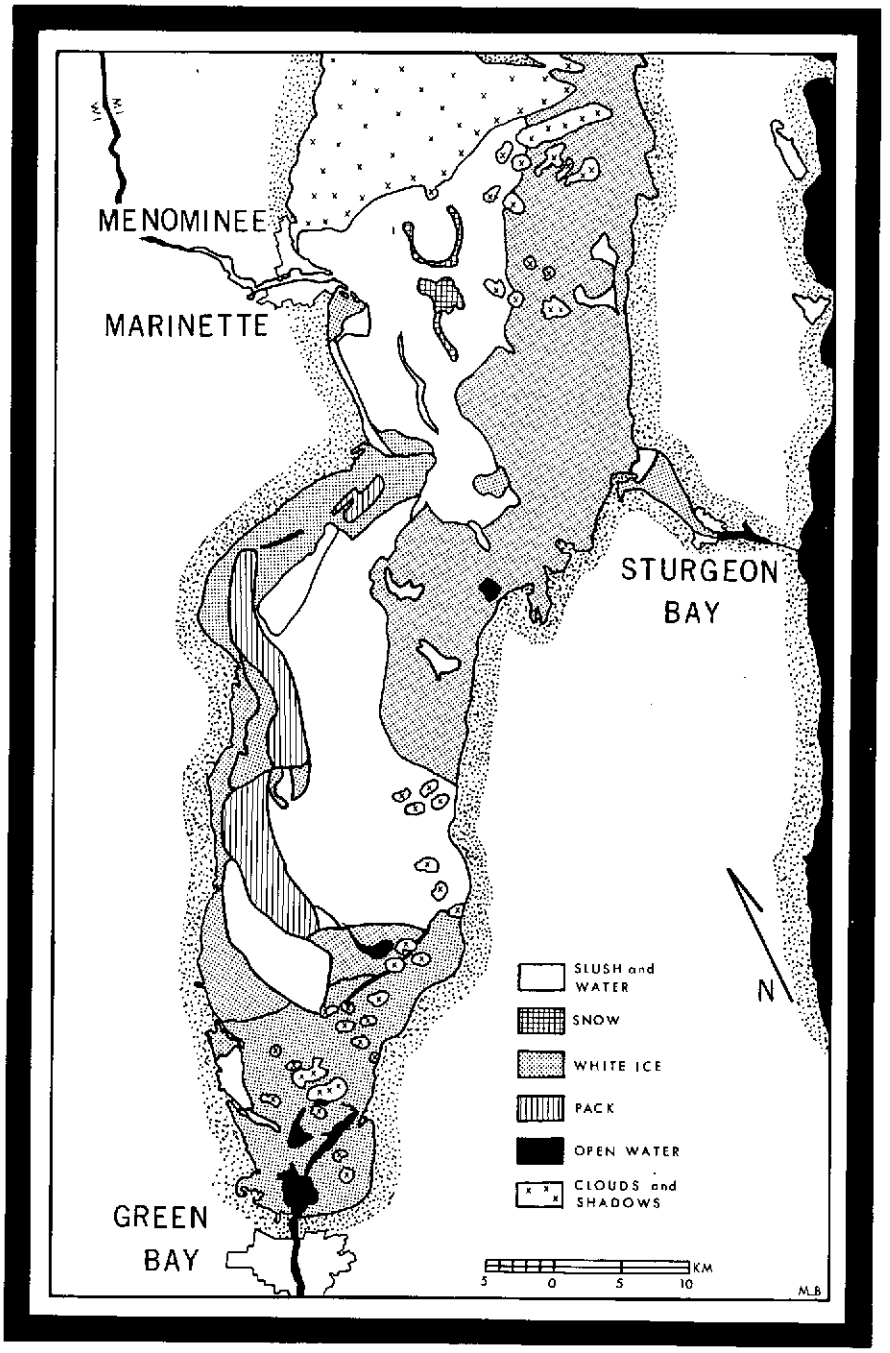

FIGURE 7. INTERPRETATION OF ERTS(I) IMAGERY FOR GREEN BAY, WI. Scene: 1197-16095.

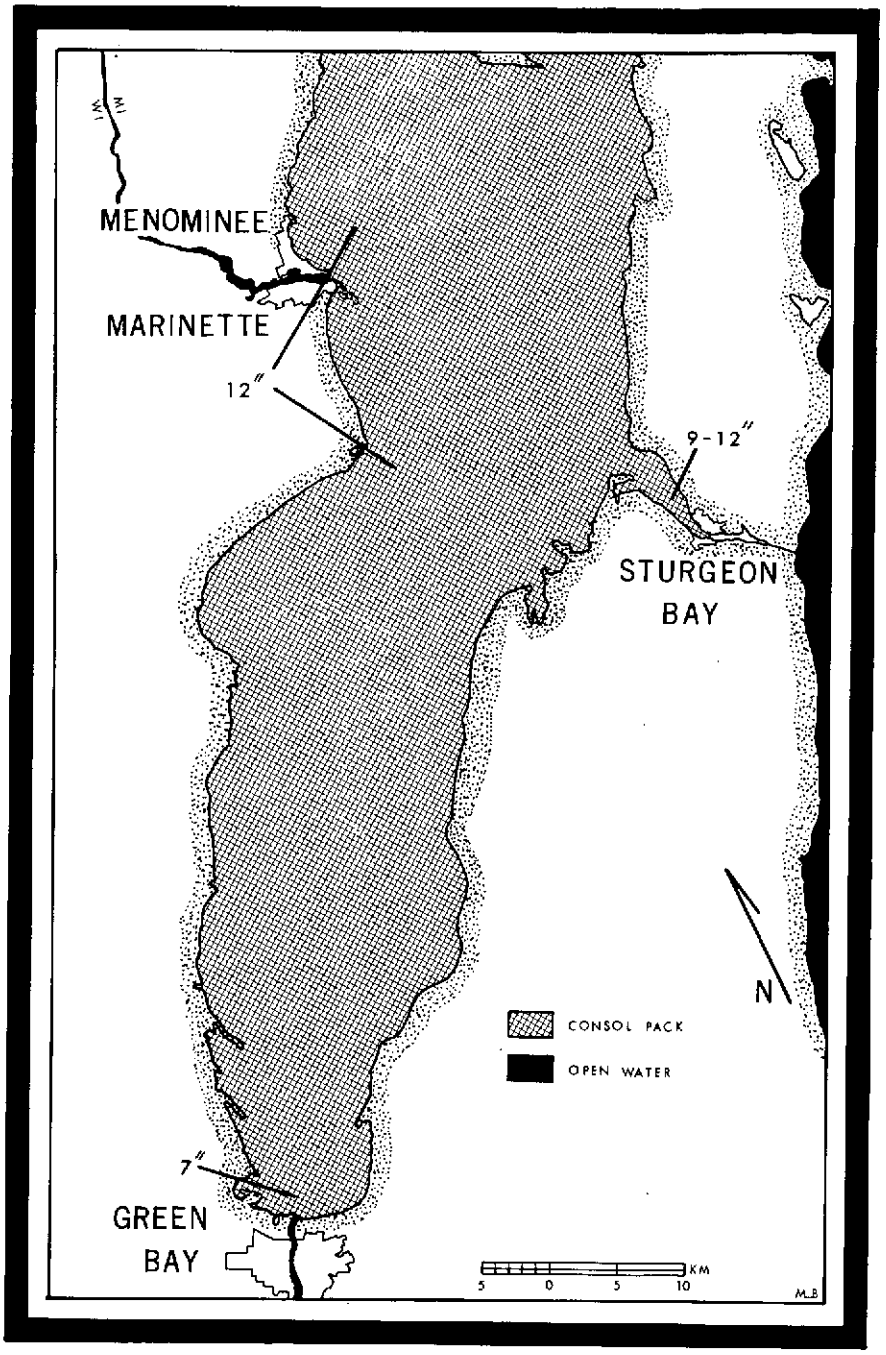

FIGURE 8. ICE ON GREEN BAY, WI. 05FEB73. (SOURCE: U.S. Survey, Detroit, MI.)

ERIM
FORMERLY WILLOW RUN LABORATORIES, THE UNIVERSITY OF MICHIGAN

ERTS(I) TYPE I REPORT

05 Sept. 1973

ERTS DATA REQUEST FORM

APPENDIX B

M. L. Bryan, #U201

Environmental Research Institute of Michigan
P.O. Box 618
Ann Arbor, Michigan 48107

TABLE OF CONTENTS

FIGURES

TABLES

I. INTRODUCTION

The development of remote sensors and their applications to earth resources has followed a series of steps resulting in increasingly complicated and sophisticated instrumentation. Following the early work using real aperture PPI scope photographs (CAMERON, 1964; FEDER, 1960) for geo-surveys, more complicated synthetic aperture side-looking airborne radar (SLAR) systems were employed for such studies (BEATTY, et al., 1965; ROUSE, MacDONALD and WAITE, 1969). An example of early imagery from the Environmental Research Institute of Michigan (ERIM) SLAR is presented in Figure 1. However, radar was still confined to one wavelength, although multiple polarizations were available. Several non-simultaneous multiple wavelength radar systems were also developed. The Naval Research Laboratories (GUINARD, 1971) developed a four wavelength radar and the Willow Run Laboratories of The University of Michigan (PORCELLO and RENDLEMAN, 1971) developed one operating on two wavelengths, each with like and cross polarization.

Nonetheless, the development of a non-simultaneous multifrequency radar did not answer all of the demands of some authors in the radar/earth applications literature (e.g., MOORE and THOMANN, 1971, SIMONETT, 1970). The statistically valid identification of various types of resources and land use categories was considered to be almost impossible when data were confined to one or even two wavelengths which were not simultaneous. Results available (LUNDIEN, 1965; HAGFORS, 1967) show that measurements with multiple wavelength, multipolarization sensors increase the validity of the identification. However, large amounts of data

FIGURE 1. RADAR IMAGE OF LAKE ERIE SHORELINE. X-Band (HH). 50 × 50 ft Resolution. 1960.

require automated processing if interpretation is to keep pace with data collection, especially with the advent of satellite borne side-looking radars. One of the problems with the automatic data processing technique is the need for image registration so that corresponding locations of any set of images are congruent. For example, the four images shown in Figure 2 are not congruent. These four images (X-BAND, HH and HV; L-BAND, HH and HV)[1] were not obtained simultaneously. Different antenna depression angles and alterations in aircraft flight lines (and consequently, the imaged areas) occurred between the X-BAND and the L-BAND flights.

The Environmental Research Institute of Michigan has recently developed a multifrequency, multipolarization simultaneous SLAR system operating at both X-BAND (3.2 cm.) and L-BAND (23 cm.) This work was supported by NASA contract No. NAS9-12967. Generally, this instrument operates in the HH or HV mode, but it can also be configured to operate in the VH or VV mode. The question of registration is not totally dependent on the existence of a simultaneous radar set as described. The entire radar system (e.g., transmitter and receiver, recorders, optical processors, etc.) also must be considered. These sources of possible error are not, however, the subject of this report, and it is tacitly assumed that, for these items, "all things are considered equal."

1. HH refers to Horizontal transmit, Horizontal receive. Similarly for HV, VH, VV.

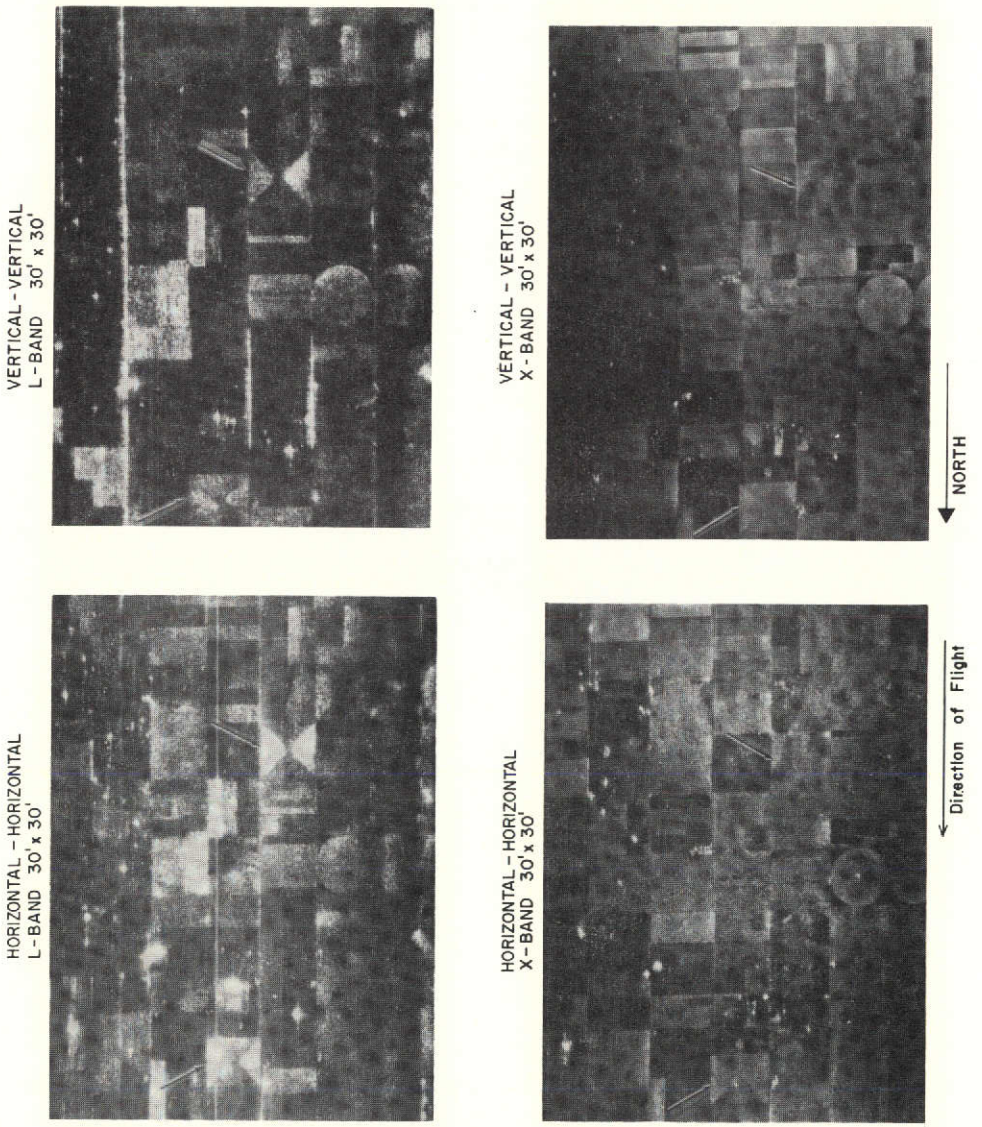

FIGURE 2. FOUR CHANNELS OF SLAR IMAGERY — (NON-SIMULTANEOUS)

II. INSTRUMENTATION AND FLIGHT PROGRAM

The multiplexed synthetic aperture side-looking radar was mounted in a C-46 aircraft. This radar operates at X-Band (3.2 cm) and L-Band (23.0 cm) wavelengths, transmits horizontal or vertical polarization and receives both horizontal and vertical polarizations. Hence, a set of four images from four channels X(HH,HV) and L(HH,HV) are generated. All four channels were operative at the time of the imaging passes, but as indicated in Table 1, all channels for all areas have not been processed (in the final mode) and cannot be discussed in this report.

	Preliminary Processing				Final Processing			
	X BAND		L BAND		X BAND		L BAND	
SWATH	HH	HV	HH	HV	HH	HV	HH	HV
A								
B								
C							X	X
D								
E								
F			X	X				
G			X	X				
H			X	X				
I			X	X				
J			X	X				
K			X	X				
L					X	X	X	X

TABLE 1. Completed Final Processing for Multiplexed Radar Imagery of 5 April 1973. (30 x 30 ft Resolution)

The eight imaged areas are outlined in Figure 3. Sites B and L are in eastern Michigan, bordering on the western portion of Lake Erie. The land here is quite low and, due to the excessive northeast winds

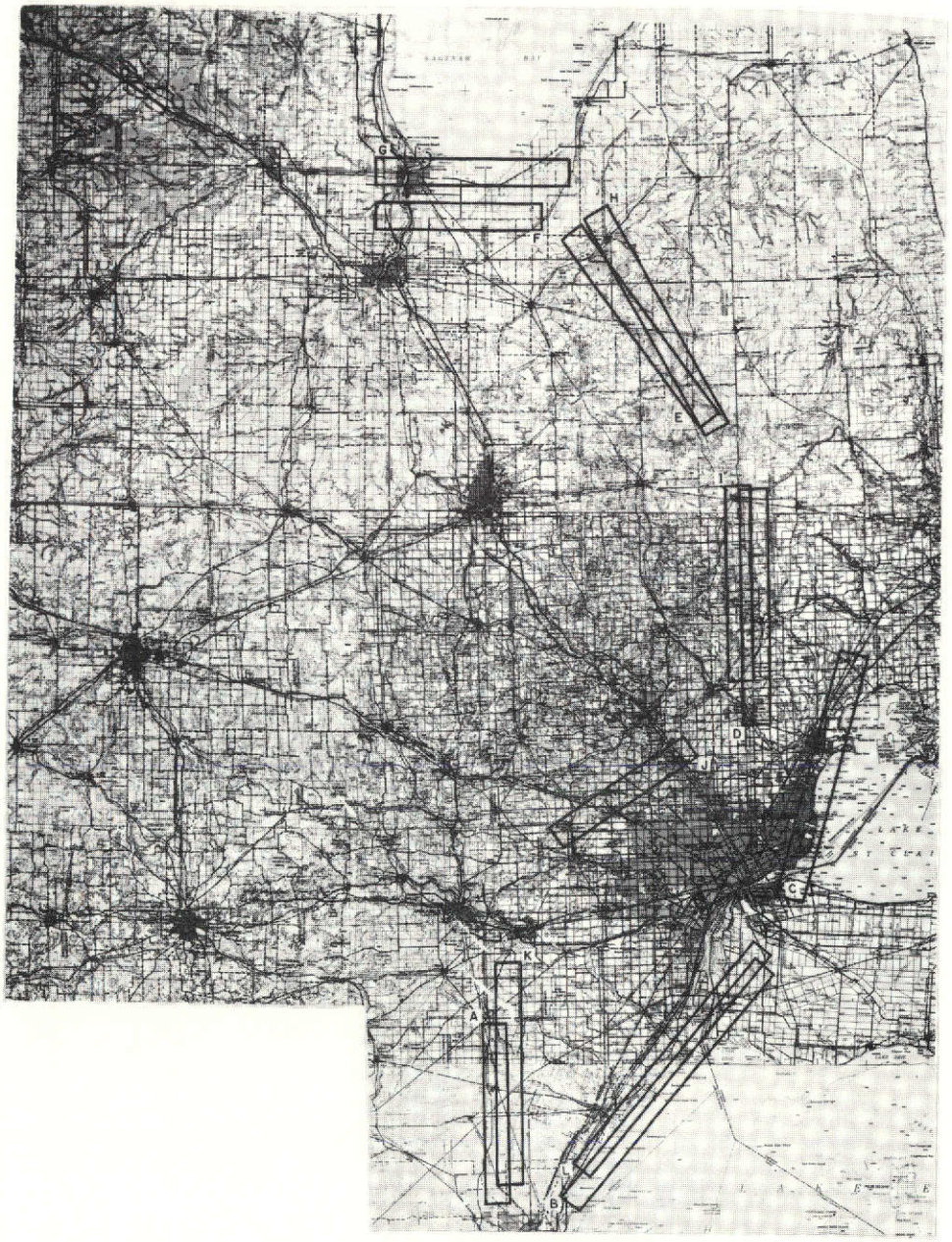

FIGURE 3. AREAS IMAGED, X-L IMAGING FLIGHTS. 05APR73.

immediately prior to the imaging data, many businesses and residences were flooded. Site C is a highly developed northeastern suburb of Detroit and bordering on western Lake St. Clair. Portions of this area had also experienced flooding for several weeks prior to the imaging flights. Sites D, I, E, and H were selected because of considerable interest in the Michigan Department of Highways for collection of data concerning environmental assessment of areas in which the development of major highways was being considered. These areas were imaged because they were along the flight paths between the southern to the northern flooded areas. Sites G and F are the 'northern flooded areas' along the southern end of Saginaw Bay. These areas are quite flat, topographically low and covered by an extensive network of drainage ditches. Floods at the time of the flights were primarily the result of strong northeasterly winds which raised the water levels along the shoreline to as much as 12 feet above the norm. The floods were so severe that portions of both the southern and the northern areas were later designated as disaster areas and relief monies were made available to residents and business enterprises in the affected areas.

Table 2 shows the aircraft flight parameters during the imaging passes. In all cases, the radar is looking to the right of the aircraft. A total of 1023 square miles were imaged over a distance of 341 linear flight miles. Flight altitudes varied between 4.6 to 7.5 thousands of feet with an average stand-off range of 12-14 thousands of feet.

SWATH	A/C ALTITUDE (FT X 1000)	STAND OFF RANGE (FT X 1000)	LENGTH OF PASS (MILES)	LOOK DIRECTION	DEPRESSION ANGLE NEAR	FAR
A	7.5	14	23	W	20°	11°
B	7.5	14	39	SE	20°	11°
C	7.5	14	37	E	20°	11°
D	5.6	12	29	E	30°	10°
E	5.6	12	29	NE	30°	10°
F	5.6	12	21	N	30°	10°
G	5.25	12	24	S	14°	7°
H	4.6	12	31	SW	14°	7°
I	5.6	12	34	W	14°	7°
J	5.6	12	20	NW	14°	7°
K	5.6	12	27	W	14°	7°
L	5.6	12	37	SE	14°	7°

TABLE 2. Flight Parameters for Imaging Runs.

III. IMAGE INTERPRETATION

Two sets of imagery are included in this report - one is primarily urban the other rural.

A. RURAL AND SUBURBAN AREAS:

Figure 4 illustrates the area which was imaged in Pass L during the 5 April 1973 multiplexed radar flight. As shown in Table 2, this area is approximately 37 miles long and has an average swath width of 3.5 miles, for a total of approximately 130 square miles. The aircraft was flying northeasterly, and the look direction is southeast toward the lake. Depression angles varied between 14 degrees (near range) to 7 degrees (far range) for this pass.

One portion near the center of the imaging run illustrated in Figure 4 has been selected for this brief interpretation. Four channels

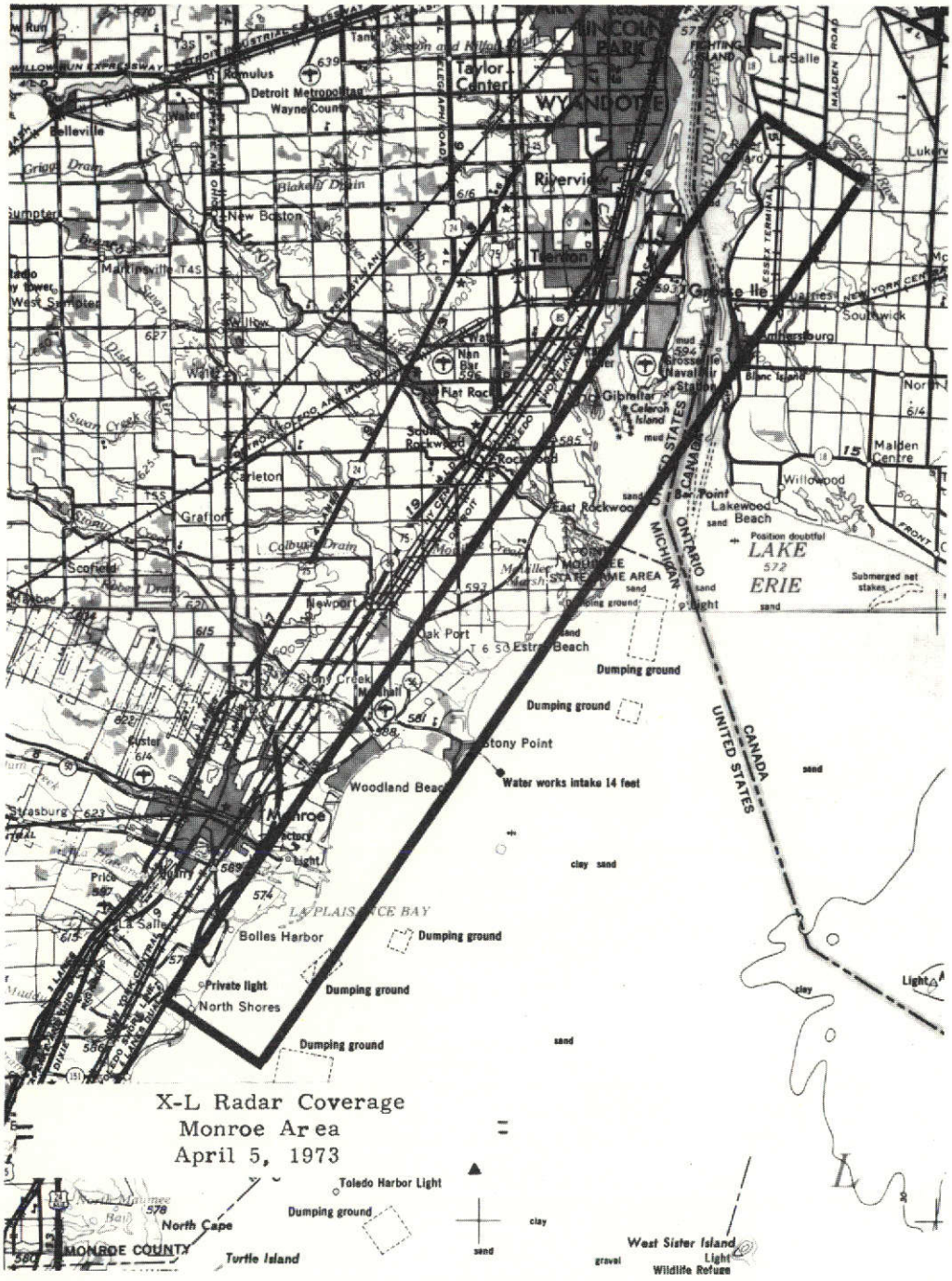

FIGURE 4. X AND L RADAR COVERAGE SWATH L. Southeastern Michigan. 05APR73.

(Figures 6, 7, 8, and 9 respectively) of radar imagery are shown. A detailed map view of the selected area is given in Figure 5. This discussion will concentrate on three major groups of features: hydrological, vegetative and cultural.

1. Hydrological:

The dominant hydrologic features of all four images are Lake Erie and Swan Creek.

Much of the land along the Lake Erie shoreline is quite low and identified on the topographic map (Figure 5) as swamp or marsh. Such areas, as in Zone 6H, are most easily identified on the X(HH) image although they can be identified with considerable ease on all four channels. The central portion of this marsh has assorted vegetation (grasses, reeds) extending above the level of the water. These vegetative zones are most clearly seen on the X(HH) and L(HV) images as light areas in the middle of the darker surrounding water (specular reflection from smooth water is directed away from the radar). Their existence would be speculative based upon only the L(HH) interpretation, and they would be missed entirely if only the X(HV) were used for interpretation. Figure 10 is an aerial photograph (oblique) of this marsh.

Zone 3H, as indicated in Figure 9, is a low lying field which has been drained by several ditches on its northern, eastern and southern sides. It is bordered immediately to the southeast and east by marshes. This field, as indicated on the radar image, has been flooded, an event which would be expected given the elevation of the field at its western end (574-576 ft.), which is, according to the topographic map, only 2 - 4

FIGURE 5. INDEX MAP FOR SLAR IMAGERY. Portion of Swath L.

FIGURE 6. X-BAND (HH) SLAR IMAGE. Portion of Swath L. 05APR73.

FIGURE 7. X-BAND (HV) SLAR IMAGE. Portion of Swath L. 05APR73.

FIGURE 8. L-BAND (HH) SLAR IMAGE. Portion of Swath L. 05APR73.

FIGURE 9. L-BAND (HV) SLAR IMAGE. Portion of Swath L. 05APR73.

FIGURE 10. MARSH IN ZONE 6H. Looking southeast from approximately 1000 ft (AGL). (Original: 35 mm Kodachrome slide.)

feet above the level of Lake Erie. Several additional fields immediately to the north, in Zone 3F also have been flooded.

The small community of Estral Beach suffered some flooding during this period, as might be suggested by the H(HV) image (e.g., Zones 4H and 5H). Although many areas of very low return, possibly indicating specular reflection by water surfaces, are present, it is not definite that the many low returns are the result only of flooding. Some fields, as in the northwestern corner of Zone 4H show some slight returns, with an intensity not unlike that seen in Zone 6H from the marsh mentioned earlier. It might properly be concluded that this area is also one which has been inundated, but in which the vegetation is slightly above the surface of the water. By comparing the same zone with the marsh and weeds in the L(HV) image, we do not detect the slight L-Band return. Consequently, we can infer that the vegetation at this place is either more sparce or shorter, thereby appearing smoother at the longer (23 cm) L-Band wavelengths. This is a commonly understood aspect of the use of dual wavelength active microwave sensors, that is, the effect of roughness on backscattering, and one which has been documented in numerous articles (e.g., COSGRIFF, PEAKE and TAYLOR, 1960). Given a roughness of magnitude ℓ; an L-Band wavelength of λ_L and an X-Band wavelength of λ_X then:

$\lambda_L > \ell$ and $\lambda_X > \ell$ both images will have smooth textures

and for:

$\lambda_L > \ell > \lambda_X$ L-Band image will appear smooth
X-Band image will appear rough.

Within the community of Estral Beach, we observe a series of buildings (residences) along the beach ridge in Zones 4H and 5H. Landward of these homes is a linear area of no return which is a canal or drainage ditch as indicated on the topographic map. The main area of the town (Zone 4H) is both topographically low and one of very erratic radar returns. Such returns could be the result of a combination of backscatter from the tops of relatively sparce deciduous trees and from water surfaces. Although it was first speculated that large portions of the community were flooded, it was found that these low returns were primarily the result of both short cropped and mowed lawns surrounding the residences, and water, the former being dominant. The water in the town was the result primarily of precipitation and high ground water tables rather than the influx of lake waters.

One item of particular interest is that it apparently is not possible to predict the spatial distribution of the flooding waters from elevation contours.[2] This is seen, for example, in the large field (Zone 3H) containing the 575 foot contour which was entirely flooded. To the west, the same elevation (and a continuation of the same contour line) is not inundated. Even though the wooded area was in standing water, the suggested extension of the wet, saturated and inundated land to the west of the woods is not even closely congruent with the contour lines. This problem of determining flooded areas requires additional and intense

2. Distribution of floods as determined by contour lines is the technique being used by the U.S. Department of Commerce (National Oceanic and Atmospheric Administration) in their new map series - "Storm Evacuation Maps" initiated this year.

study if radar is to be used as an aid in flood mapping and research.

Finally, a small creek in Zone 10G, draining eastward into Lake Erie is most easily outlined on the X(HH) image. Likewise, Blanchett Drain, flowing into Swan Creek (northeast corner of Zone 8E) can be traced upstream a slight distance on all images, but most easily perhaps on the X(HV) image. In this case, however, it is not the drain per se which is being traced, but rather the high reflectivity of the vegetation which aligns the bank of the drain. The same phenomenon can be seen along other streams in the images.

2. Vegetative:

Deciduous trees, bushes and shrubs which were in the process of budding (only a few trees and essentially no bushes retained last year's leaves) are clearly seen on all four images. For example, the wooded area already mentioned in Zone 4F are more apparent and, to a certain degree, more prominent on the L-Band imagery than on the X-Band. It will be recalled that most of this wooded area was standing in water. However, there is no suggestion of that in the imagery when we compare this area with other wooded areas. This indicates that there is effectively no penetration of trees at these wavelengths and that the backscatter is being controlled primarily by the tree crowns or the tree volumes.

Much effort has been extended by other researchers in using the non-simultaneous SLAR as an identification instrument for crops, (e.g., HARALICK, CASPALL and SIMONETT, 1970), but the accuracy of identification is still

quite tenuous.[3] Texture, tone, spatial distribution - interpretation parameters transferred to SLAR imagery from aerial photography - are all used in attempts at visual interpretation. For example, radar texture of the field in the northeastern portion of Zone 11D is, for the X(HH) image, quite smooth. Corn stubble covers approximately 60 per cent of this field and has an average height of 1 - 2 feet. Although each of the four images gives a different texture and tone for this field, not all fields with this crop type give a similar tone and texture for a given wavelength and polarization. The precise reasons for this particular case have not been determined, but several factors, including spacing of the crop, the orientation of the crop rows relative to the radar look direction, different heights (and therefore roughness) of the crop, and processing errors may all contribute in part to this variation in visible return. This is not to say, however, that multiple radar images are not of utility in visual image interpretation, for indeed they are.

Much work needs to be conducted if we wish to identify vegetative features using SLAR systems as the primary data collection instruments. Problem oriented experiments, both theoretical and empirical, need to be designed and conducted to adequately study the interactions of radar radiation and the several earth surfaces (land uses), especially as concerns surface roughness, moisture and vegetation variations. Also, much of the existing literature on radar interpretation, especially when the more

3. Most of this previous work concerning vegetation indentification using SLAR has been conducted using Ka-BAND (0.8 cm wavelength) real aperture radars.

subtle features are being discussed, should be thoroughly scrutinized and critically evaluated prior to the development of such programs.

3. Cultural:

With one exception, the cultural features visible on this imagery are quite common. Dixie Highway trends to the northeast across the western portion of the image (Zone 8A to Zond 1D) and is clearly seen on all four images. Its route is, however, less prominent on the L-Band images than on those of the shorter wavelength. The bridge, where this highway crosses Swan Creek (Zone 8A) is most prominent on the X-Band (HH) image, but is also visible on the other three images. The area around this bridge is a small village of Oldport, Michigan, and especially on the L-Band images it is quite prominent. Figure 11 is an oblique aerial view of this site.

One problem which does occur in such areas of concentrated cultural features is their tendency toward 'blooming' on the L-Band, thus obscuring many adjacent features. On the other hand, this same feature greatly enhances isolated cultural features and presents them quite prominently, especially if they are located in an area of otherwise relatively low returns. For example, the several buildings in the vicinity of Zone 6E are strongly emphasized on the L-Band images. This enhancement is much greater for man-made objects, with their right angles and planar sides, than for isolated trees and aids somewhat in the visual discrimination between these two types of features.

The shoreline area to the south of Swan Creek is one which has undergone considerable development. In this area (Zones 8H, 9H, 10H)

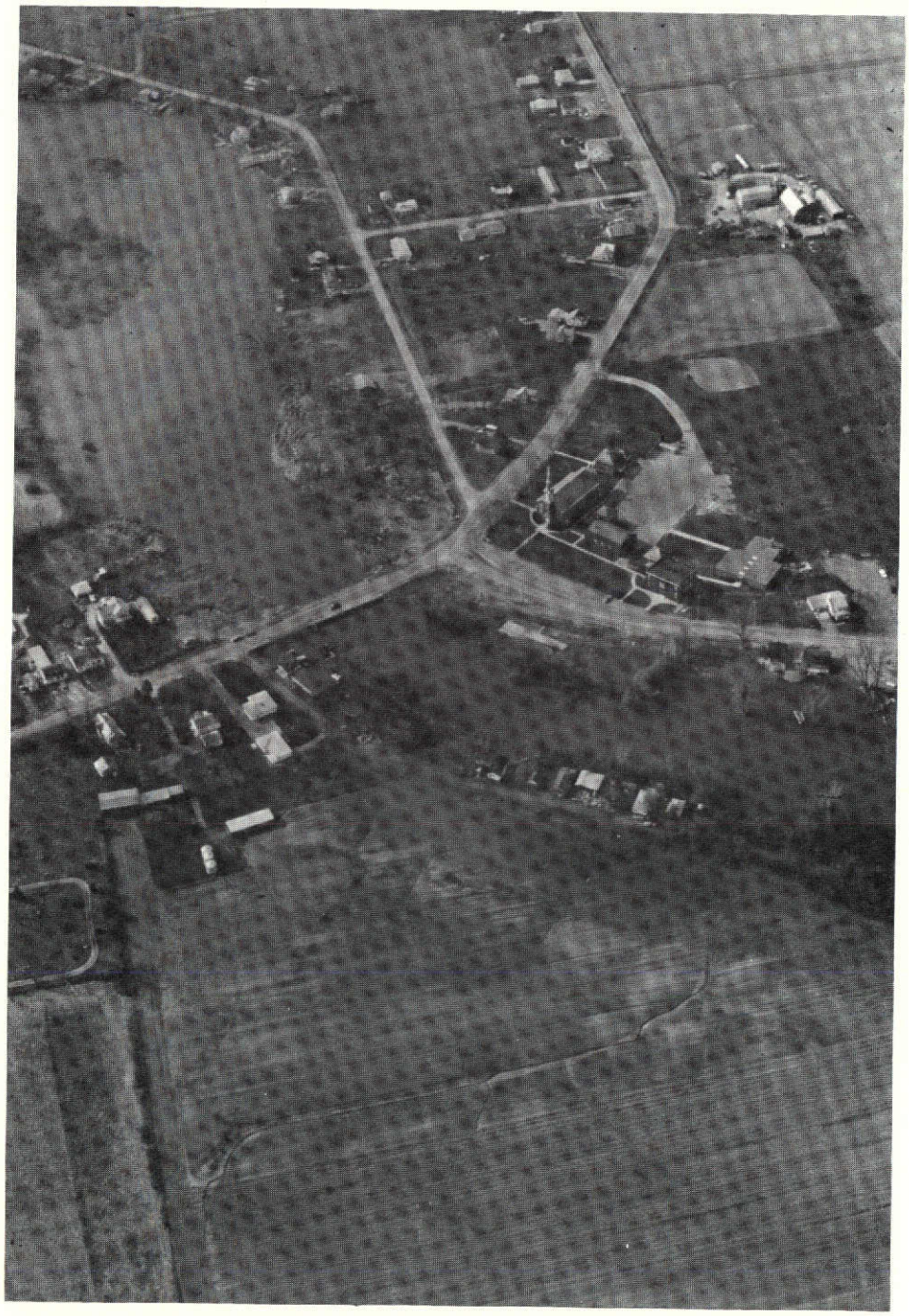

FIGURE 11. VIEW OF THE COMMUNITY OF OLDPORT, MI. AND THE DIXIE HIGHWAY BRIDGE ACROSS SWAN CREEK. Looking south from approximately 1000 ft. (AGL). (Original: 35 mm Kodachrome slide.)

is the location of the Enrico Fermi power plant. The very high reflections, especially prominent on the L-Band (HV) image are from the main plant (Zones 10H and 10I) whereas the small circle (Zone 9H) nearer to Swan Creek and prominently viewed on all images except the L-Band (HH) (on which it is somewhat obscured, but sill visible) is a cooling tower which is being built. Another cooling tower also in Zone 9H to the south of the first is not clearly visible on any image, However, it may be inferred especially on the X-Band HH image by its shadow which is quite prominent toward the shoreline. Figure 12 is an aerial photograph of these two cooling towers and the surrounding terrain.

A new road (clearly seen on the two X-Band images) has been built between the Dixie Highway and the Enrico Fermi plant. This road is one of four communications facilities (from southwest to northeast, in order - utility poles, road, railroad, electric transmission line) connecting the plant and Dixie Highway. The road is most easily viewed on the X(HH) and X(HV) images whereas the utility line appears as groups of three dots spaced about 4 times farther apart than the utility poles on the opposite side of the road. The railroad is most easily identified on the X-Band HV image, but is also distinguishable on the X-Band (HH) image. Reference to Figure 5 indicates that, in Zones 11D and 11E, the transmission line crosses the railroad and is presently on the southern side of the latter. This is not indicated on the X-Band images, but is seen most prominently on the L-Band HH image.

By including all four images during the interpretation, the increased detail and information may, in an absolute sense, be relatively slight.

FIGURE 12. LOW OBLIQUE AERIAL PHOTOGRAPH OF THE COOLING TOWERS, ENRICO FERMI PLANT. Lake Erie in the foreground. Looking generally southeast from 1000 ft. (AGL). (Original: 35 mm. Kodachrome slide.)

However, the significance of this increase can be paramount, depending upon the nature of the investigation. The obvious example is, of course, the previously discussed power line.

Consequently, the nature of the problem to be studied dictates, to a certain degree, the wavelength and polarization which is to be most advantageously employed when collecting SLAR imagery. The use of all four channels, which can now be economically collected with one aircraft pass, allows the interpreter to extract a much wider range of detail and topics from the SLAR imagery than has heretofore been possible.

B. URBAN AREA:

As noted in Table 1, for Swath C, only the L-Band imagery is available. The small scale map (Figure 13) gives the general location of the study area while a section of the 1:24,000 USGS topographic quadrangles (Mt. Clements, East; Mt. Clements, West) of the study area is included in Figure 14. Figures 15 and 16 present the L-Band (HV) and (HH) imagery, respectively.

Again, water bodies dominate a large portion of the image. Lake St. Clair is shown in the southeastern portion of the image. The northern quarter of the study area is the Selfridge Air Force Base, also one of very low radar returns. The base is composed primarily of runways, aprons and taxiways with grass areas between them. Some of the control towers (Zone 1F) and isolated bright point targets are visible - the latter are presumed to be vehicles or aircraft momentarily stationary on the runway area.

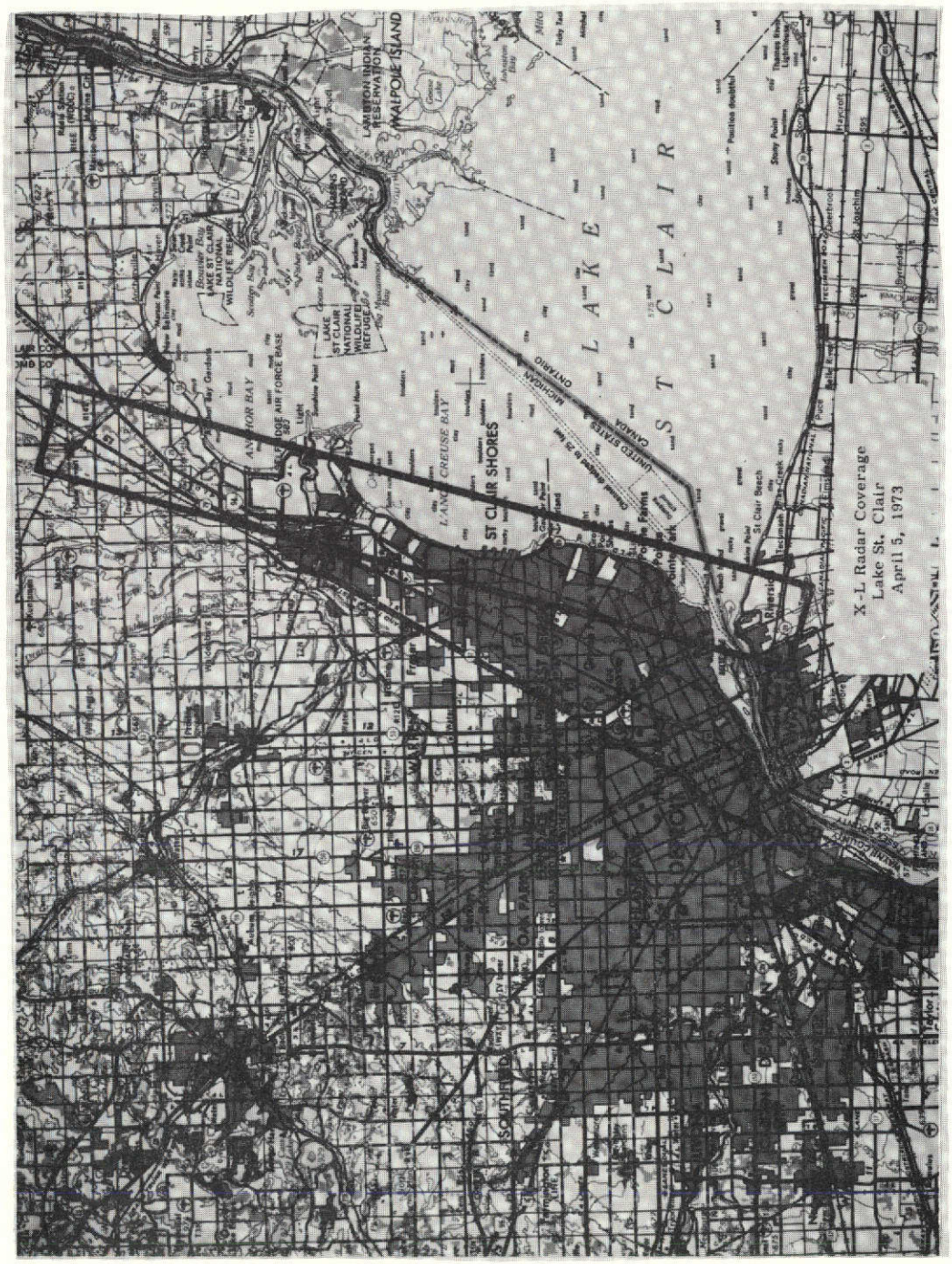

FIGURE 13. X AND L RADAR COVERAGE, SWATH C. St. Clair Shores, MI. 05APR73.

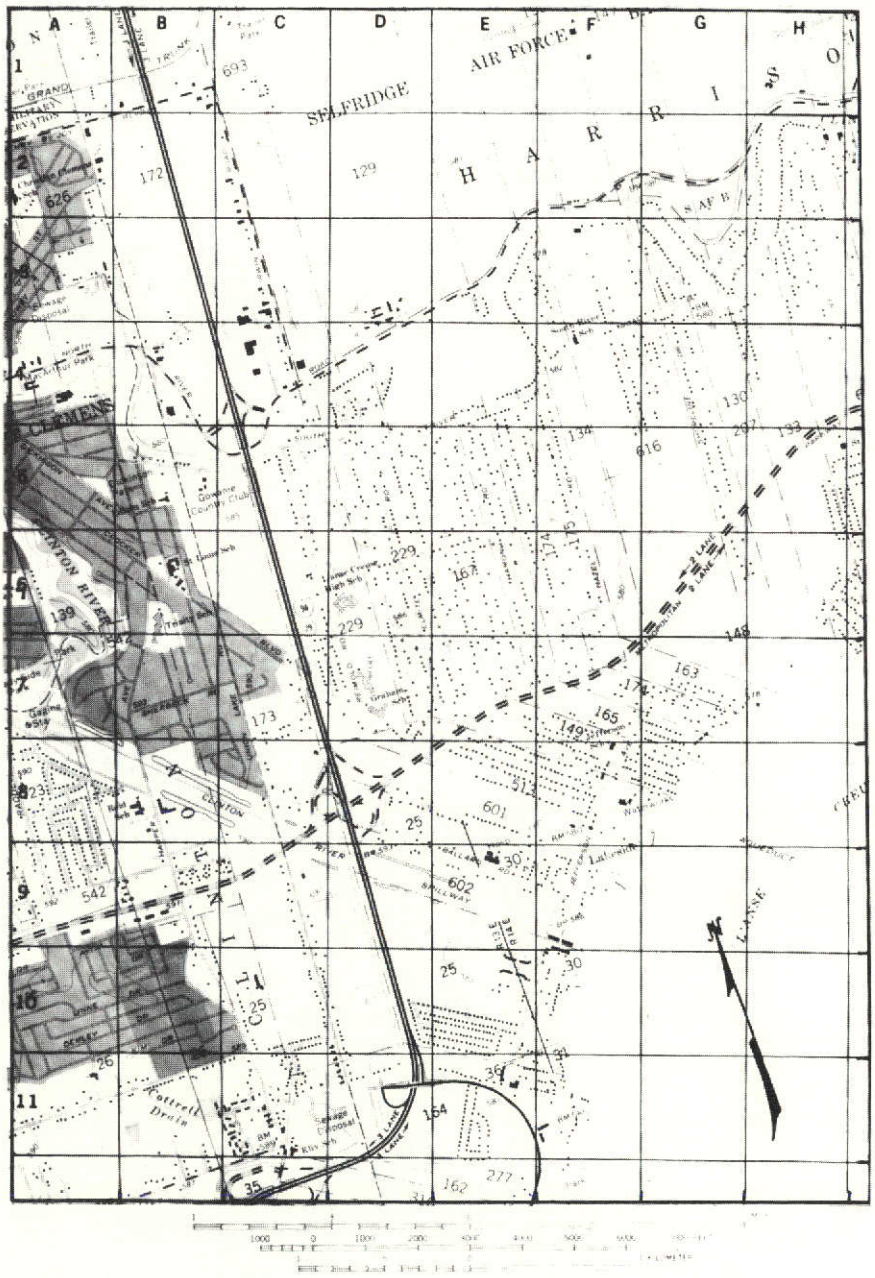

FIGURE 14. INDEX MAP FOR SLAR IMAGERY. Portion of Swath C. 05APR73.

FIGURE 15. L-BAND (HV) SLAR IMAGE. Portion of Swath C. 05APR73.

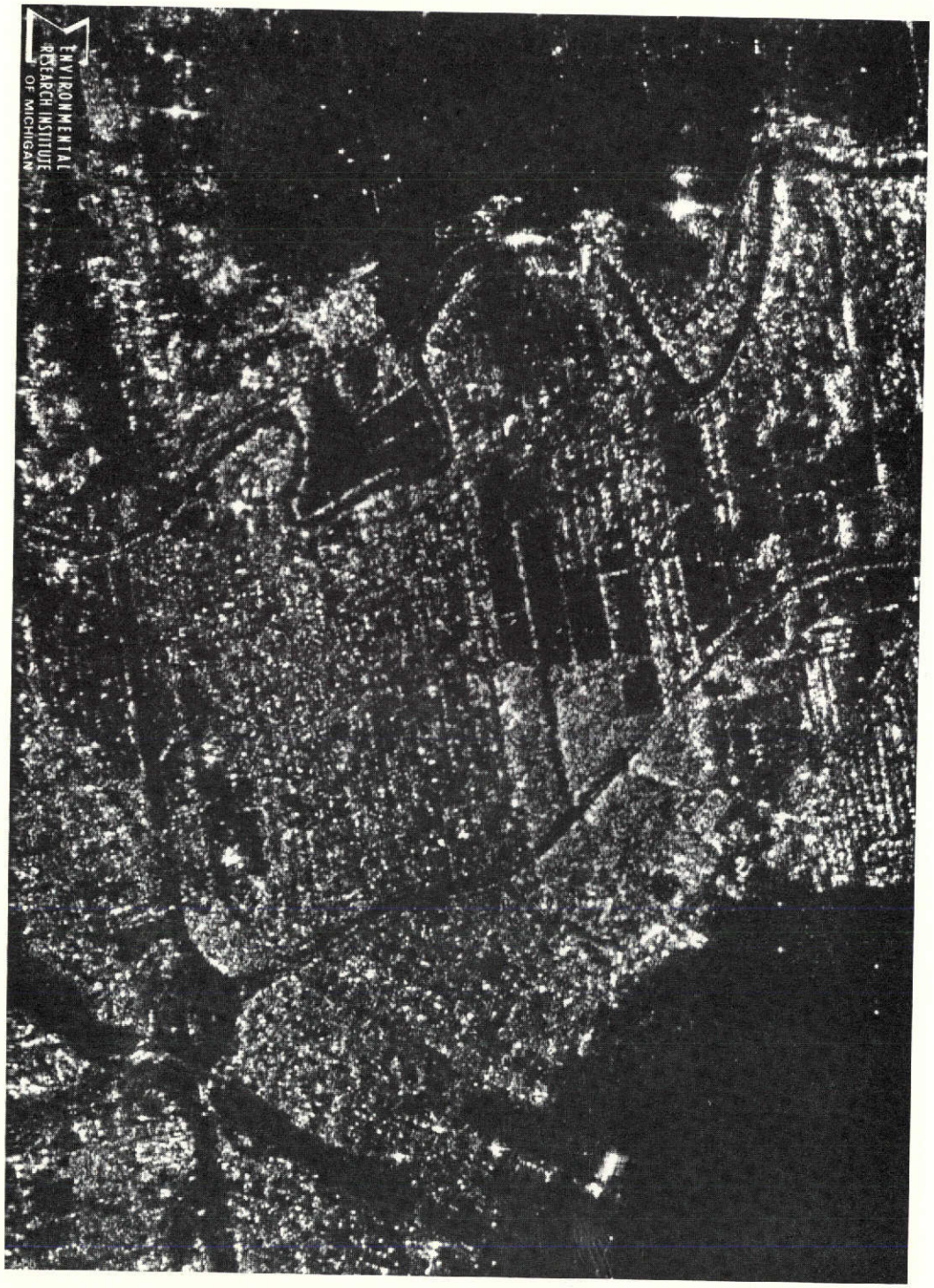

FIGURE 16. L-BAND (HH) SLAR IMAGE. Portion of Swath C. 05APR73.

The meandering course of the Clinton River is easily identified on both images, and, to a certain degree, it has the appearance of being more precisely defined on the L(HV) image. This is caused by the lower signal level in the L(HV) image and therefore the lower 'blooming' of the trees. This is true of all features, both cultural and natural, as seen on the HV images of this pass.

Two large linear patterns are apparent on the images. The first feature is the freeway system which runs generally NS/EW and forms a fairly large interchange in Zones 8C/8D. The system was planned when the topographic map was prepared (1968) and had been completed at the time of the radar imaging. Because the concrete covered bridges tend to be poor radar reflectors, the highway interchange is suppressed in the radar image. Had the image been made prior to the covering of the steel with concrete, the interchange would have provided a very bright return, similar to that of the cooling tower which was under construction at the Enrico Fermi plant (Figure 12). Moving vehicles are suppressed by synthetic aperture radars and hence there is an absence of bright point returns from vehicles travelling the interstate system. This image is similar to other radar images from Interstate Highway and freeway interchanges and systems.

A second feature is the Clinton River Spillway which enters Lake St. Clair (L'Anse Creuse) in Zone 9F. This spillway is generally bordered by smooth surfaces and appears on the imagery much larger than the water surface is in reality. The smooth surfaces present a specular return not unlike that of the actual spillway water surface and consequently the

specific determination of the spillway dimensions is indeterminable.

Much of the remainder of the image has land uses which are both residential, recreational (parks) and institutional (primarily schools and hospitals). Areas of thick deciduous vegetation (e.g., 6F) are clearly identified and differentiated from other areas of the city which are composed of older residential areas. This is illustrated in Zone 10A where the deciduous trees are interspersed with streets and homes. In this area, the texture is somewhat more variable, reflecting the greater variation in the surface as reflected to the radar.

Variations in the orientation of the city street patterns are identifiable in both of the images. Especially in Zone 10A and 5A we are able to note both of the primary (orthogonal) street patterns, although neither is oriented directly with or normal to the look direction of the radar energy. The importance of look direction in identifying linear cultural features has been discussed by Lewis, MacDonald and Simonett (1969), in which they note that for different types of features (e.g., railroads), a non-orthogonal look direction reduced the possibility of correct identification (incidentally, polarization is also greatly influences detectability of cultural features). Conversely, orthogonal look directions often enhance the accurate identification of some cultural features. Obviously, a study of such dependencies should be undertaken prior to planning radar imaging flights over areas having a large number of cultural features.

There are almost no cultural features which are aligned to reflect specularly toward the radar. This is because the orientation of the

radar was not directly orthogonal to the primary street patterns of the imaged area, and consequently the 'cardinal effect' is minimized by this aspect angle, in combination with the long wavelength of the L-Band radar. Some bright point returns are noted. Specifically, L'Anse Creuse High School (Zone 6D), some control tower facilities at the Selfridge Air Force Base, and the facilities off-shore from the waterworks plant in Zond 8G. This latter is especially prominent in the HH image and occasionally other such bright point returns are visible on the HH but not the HV image (e.g., Zond 10D). This is related to the signal levels of the radar, as mentioned earlier.

The interpretation of such cultural areas as the area of St. Clair Shores, Michigan, is often in doubt and needs further study. It is pointed out that, although some publications are available for guidance in such studies (e.g., LEWIS, 1968; PETERSON, 1969), the full potential of this fairly versatile remote sensor has not been properly exploited for extraction of urban data.

IV. CONCLUSION:

This paper has briefly pointed out some of the variations in return and some interpretation potentials when employing the simultaneous, dual-frequency, dual polarization side-looking airborne radar for the study of the earth's surface. The purpose of this report is to provide a preliminary statement of the output of such an instrument which was recently developed by ERIM and, at the same time, to present some basic interpretation. However, due to cost limitations the ground truth for definitive identification of the features has not been conducted. Conse-

quently, this report is not conclusive. However, it is apparent that even at this level of interpretation, the use of four channels (two wavelengths, two polarizations) allows superior interpretation and additional inferences over those which would be available if only one wavelength and one or two polarizations were used.

V. ACKNOWLEDGEMENTS:

Several individuals of the ERIM Radar and Optics staff have contributed markedly to the preparation of this statement concerning the multiplexed radar system. Mr. Ben Drake, Dr. Philip Jackson, Mr. Richard Larson, and Mr. Charles Liskow are to be specifically thanked for their review of and contributions to this paper.

VI. REFERENCES

1. Beatty, F. D. et al, 1965, Geoscience Potentials of Side-Looking Radar, Alexandria, Va., Raytheon Autometric Corp., Sept., 2 Vols.

2. Cameron, H. L., 1964. "Ice-Cover Surveys in the Gulf of St. Lawrence by Radar", PHOTOGRAMMETRIC ENGINEERING, V.30, No.5. Sept., pp. 833-841.

3. Cosgriff, R. L., W. H. Peake and R. C. Taylor, 1960. Terrain Scattering Properties for Sensor System Design, (Terrain Handbook II.) Columbus, Ohio, The Ohio State University College of Engineering. Engineering Experiment Station. Bulletin. V.29. No.3. May, 118 pp.

4. Feder, A. M., 1960. "Interpreting Natural Terrain from Radar Displays" PHOTOGRAMMETRIC ENGINEERING, V.26, No.4, Sept., pp. 618-630.

5. Guinard, N. W., 1971. "Remote Sensing of Ocean Effects with Radar" pp. 15-1 to 15-12 in:
Lomax, J. B. (ed.) Propagation Limitations in Remote Sensing, PROCEEDINGS, 17th Symposium of the Electromagnetic Wave Propagation Panel of AGARD. (NTIS #AD 736 309).

6. Haralick, R. M., F. Caspall, and D. S. Simonett, 1970. "Using Radar Imagery for Crop Discrimination: A Statistical and Conditional Probability Study", REMOTE SENSING OF ENVIRONMENT, V.1, No.2, March, pp. 131-142.

7. Hagfors, T., 1967. "A Study of the Depolarization of Lunar Radio Echos", RADIO SCIENCE, V. 2, May, pp. 445-465.

8. Lewis, A. J., 1968. "Evaluation of Multiple Polarized Radar Imagery for the Detection of Selected Cultural Features", U. S. Dept. Interior,

U. S. Geol. Sur., Interagency Report NASA-130, Oct., 56 pp. (NTIS #N69-28151)

9. Lewis, A. J.; H. C. MacDonald & D. S. Simonett, 1969. "Detection of Linear Cultural Features with Multipolarized Radar Imagery", PROCEEDINGS. 6th International Symposium on Remote Sensing of Environment. Ann Arbor, Mi., U. Michigan., Inst. Sci. & Tech., Oct., pp. 879-893.

10. Lundien, J. R., 1965. "Remote Measurement of Dielectric Constants and Conductivity for Soils", IEEE PROCEEDINGS, V.5, April, pp. 420-421.

11. Moore, R. K. & G. C. Thomann, 1971. "Imaging Radars for Geoscience Use", IEEE, TRANSACTIONS ON GEOSCIENCE ELECTRONICS, V. GE-9., No. 3, July, pp. 155-164.

12. Peterson, F., 1969. "An Urban Land Use Study of Lawrence, Kansas Using K-Band Radar" pp. 39-45a in:
"The Utility of Radar and Other Remote Sensors in Thematic Land Use Mapping from Spacecraft: Annual Report", U.S. Dept. Interior. U. S. Geol. Sur. Interagency Report NASA-140. Jan., (NTIS #N69-16255).

13. Porcello, L. J. & R. A. Rendleman, 1972. "Multispectral Imaging Radar" NASA. 4th Annual Earth Resources Review Program. Vol. 2. University Programs. Houston, Texas. Jan. pp. 35-1 to 35-18. (NTIS #N72-29327).

14. Simonett, D. S., 1970. "Remote Sensing with Imaging Radar: A Review" GEOFORUM, No.2, ppl 61-74.

15. Rouse, J. W., Jr.,; H. C. MacDonald & W. P. Waite, 1969. "Geoscience Applications of Radar Sensors" IEEE, TRANSACTIONS ON GEOSCIENCE ELECTRONICS, V. GE-7, No.1, Jan., pp. 1-19.

ERIM
FORMERLY WILLOW RUN LABORATORIES, THE UNIVERSITY OF MICHIGAN

Sixth Type I Progress Report - 1 July 1973 - 31 August 1973
Task V, Recreational Land Use - 1387
I. Sattinger, UN 225, MMC 086

Frames 1319-15471 and 1319-15474 were acquired by ERTS-1 on 7 June 1973 under cloud-free conditions. An ERTS Data Request Form for photographic and tape products of these frames was submitted on 18 July 1973. As soon as these products are received, work will continue on processing of ERTS data for analysis of recreational land and open space in Oakland County. In addition to the request for digital tape of the two frames, transparencies and prints of bulk color and precision color photographs were requested. These will be used to supplement and aid in the evaluation of the computer-processed data and to determine the utility of precision processing for accurate mapping of recreational land.

Sixth Type I Progress Report - 1 July 1973 - 31 August 1973
Task VI - IFYGL (Lake Ontario) 1384
F. C. Polcyn, UN 635, MMC 114

The last of the data required for hydrologic land use mapping and soil moisture study of the Lake Ontario Basin in August, 1972, has been received and all has been converted from digital to analog format. Single channel images from ERTS-MSS channels 5 and 7 produced on the ERIM Spectral Analysis and Recognition Computer (SPARC) show excellent detail. A scenario for recognition processing has been tentatively formulated and many procedural requirements for working with multiple ERTS frames have been outlined. Sample ratio images from data collected on consecutive days would indicate that preprocessing of the data has been very successful. Analog processing on the SPARC allowing continuous display output and automatic recognition counting has been started.

Approximating the area of the basin

Segments from eight different ERTS frames were required for complete coverage of the Lake Ontario Basin. Two elements of overlap between frames had to be corrected for more accurate estimates of basin area and for accuracy in recognition counting. Consecutive ERTS frames (north to south) have at least 10% overlap when provided by NASA. When segments of the digital tape were chosen for analog processing, not all of the overlap was eliminated. Therefore, analog segments do include some duplication of data,frame to frame (Fig. 1). This procedure is good for safe computer handling, but not very accurate for data reduction. However, due to the digital character of line numbers on the analog computer, careful refinement of line starts and stops can eliminate accurately the problem of duplication between frames.

Two problems of vertical tape boundaries will introduce more substantial errors in basin approximation. When digital tapes are converted to analog format, the right edge of the data, approximately 25 resolution elements wide, is lost. Careful gating procedure on the SPARC does not seem to result in the retrieval of these points. As a result, gaps in the data are produced between individual tapes of a single ERTS frame. This problem is of no significance at the edges of frames because of the ample overlap of data from one day to the next (37% overlap allows one complete tape to be dropped with 12% overlap remaining for the next tape). In the Ontario Basin data, seven of these thin strips of data are missing, resulting in disconnecting roads and offset shorelines, etc. That this phenomenon is not unique to this project is evidenced by sharp linear discontinuities in recognition on a similar ERTS investigation (Vincent, R. K., Task X). The estimated error introduced by this problem is loss of 3% of the data.

The second problem in accurate basin coverage is the result of non-parallel tracking of the satellite from day to day. Adjoining frame boundaries are skewed, resulting in an element for which precise correction is impossible on an analog computer with only orthogonal capabilities. The areas of overlap can be seen in Fig. 1. The simplest, least expensive, and most inaccurate technique would be to process the full width for both of the overlapping tapes in each case. This would result in a 12% of one full ERTS frame overestimation. For the area of those segments used in this research, the estimated error for such a procedure would be 15% greater than that of the procedure we have selected.

If correction by gating for individual segments is undertaken, choices of error range from small amounts of data overlapped to small amounts of data missing, or some arbitrary combination of the two. Our overriding policy in approximating the basin was to collect all of the basin area possible, even when this necessitated small areas of duplication. The resultant error was eight areas of data duplicated where skewed boundaries overlap, amounting to less than 1.3% of the total basin area (See Fig. 1). The areal error introduced here is easily corrected, but automatic recognition counts will have a measure of inaccuracy introduced by this overlap.

Another problem of basin area estimation stems from our inability to follow precisely the basin outline with present analog gating capabilities. The most flexible geometry possible for one run through an analog tape is any area which can be prescribed by the union of two rectangles, $A \cup B$, for one segment. The processing cost rises exponentially with accuracy of approximation for estimates more precise than this technique allows.

Figure 2 shows the outline of the Lake Ontario Basin as it is encompassed by the complete area of analog tape segments (solid orthogonal lines). The hatched areas are those eliminated by implementation of our gating procedure. This elimination of area outside the basin can be achieved by one pass through the tape, yet it more closely approximates the area of the basin. Again, the complete basin area is included and a maximum estimate will be attained. The broken line shows a comparable minimum estimation of basin area which will be used in calculating accuracy.

In summary, an experimental procedure for basin delineation has been chosen and is presently being implemented. Decisions concerning sacrifices of areal accuracy have been based on the assumption that it is important to inventory the whole basin, even if this necessitates duplication of small quantities of data or inclusion of contiguous areas at the perimeter of the basin.

Processing for Land Use Recognition

Land use mapping and area estimates have important applications in runoff prediction and soil moisture studies. A combination of single channel, single ratio, and multiple ratio decision is planned for use in automatic recognition mapping of the Lake Ontario Basin. The choice of technique for a particular target is being made with three considerations: 1) reports of successful recognition or useful characteristics from previous ERTS and aircraft data studies, 2) comparison of groundtruth and quadrangle maps with the sample single channel and ratio images already produced, 3) reference to theoretical possibilities through the six-digit number system devised for ratio recognition by R. K. Vincent and presented in the July, 1973, ERTS Type II report submitted to NASA from ERIM. Not all such decisions have been finalized; we are still working to improve the present recognition procedures.

In accordance with a principal objective of this research, the first recognition map to be generated will be of all open water in the Lake Ontario Basin. A proven technique for such recognition is level slicing of single MSS Channel 7 for ERTS data. We anticipate inaccuracies in recognition counts due to non-recognition of cloud covered areas over the lake, and possible false recognition of small cloud shadows over the land. Our sample ratio imagery shows elimination of clouds over the lake in ratio 6/4 (MSS Channel 6 divided by MSS Channel 4). Using Channel 7 for comparison, ratio 6/4 will be tried for standing water recognition also.

Cloud cover will be treated as a recognition class for accuracy estimates of other recognition target percentages. Simple level slicing of a single channel or ratio should be sufficient for accurate estimates. It is presently estimated that cloud cover over land in the basin is less than 5% of the total basin area.

One could predict from R. K. Vincent's six-digit numbers that bare soil, wet or dry, would be uniformly brighter than most other things in the scene in ratio 5/4. Inspection of sample ratio 5/4 shows agricultural areas which are definitely brighter than anything else in the scene. Groundtruth confirmation that these areas were indeed bare has not yet been established, but seems possible.

Land use categories for which recognition will be attempted are classed as below:

1. Open water
2. Forest (with possible subclassification)
3. Marsh (with possible subclassification)
4. Urban
   a. High density (downtown) (near completely impervious)
   b. Older residential
   c. Newer residential
5. Bare soil, possibly exposed rock
6. Agriculture (with possible subclassification)
7. Pasture-grasslands

Ratios will be used in preference to single channels when a choice exists. A test class, possibly forest, will be chosen for recognition by both the best single channel and the best ratio. The purpose of such a comparison is to test the recognition extension across the scene and frame to frame.

In summary, definite recognition procedures for some targets have been established and techniques for others will be defined. Training sets in areas known by groundtruth and other backup work will be established, and recognition will be applied universally to all segments on that basis. Complete success would result in accurate, strong recognition for the whole basin without the addition of corrective values from segment to segment. The inability to recognize like-areas from one side of the basin to the other would indicate extension difficulties uncorrected by data preprocessing which must be overcome for this procedure to become operational.

Preliminary Data Quality Indications

The quality of single channel and ratioed analog imagery already produced indicates that atmospheric corrections have been successful in normalizing the many ERTS images used in this project. Individual dark levels were chosen for each ERTS frame according to the value of the darkest object in the scene. This procedure set the darkest points in each frame to the same value for processing. The resultant ratio images, run at the same gain for all frames, are of uniform quality. Overlapping tape segments collected on two different days are apparently identical.

Supportive Data Collected

Daily weather maps for the Lake Ontario region for the period July 31, 1972 to September 3, 1972 have been obtained from the U. S. Department of Commerce,Environmental Data Service.

The Albany, New York, office of the United States Geological Society was contacted for an update on the status of the hydrometric stations in the Lake Ontario Basin.

Data Quality

A strong peak in the voltage associated with the fillbits at the left edge of the first tape and right edge of the fourth for each frame causes difficulty in collecting the adjacent data. If left in the scene it will adversely affect recognition counts; if gated out, some of the data is lost. Luckily, in the Lake Ontario processing, overlap of data allowed the elimination of this phenomenon with careful gating. However, such a feature is a potential problem for other investigations.

Conclusion and Projection of Progress

Many of the problems involved with processing multiple ERTS frames have been overcome and data is in final form for analysis. The work to be performed on the Spectral Recognition and Analysis Computer (SPARC) is in progress. Once all the data is processed, to be completed in the next weeks, recognition maps for the complete basin will be generated, accompanied by areal percentages for each target. Careful analysis of experimental error and estimates of accuracy will be necessary. Also, the quality of recognition across the scene will help determine the applicability of these laboratory techniques for future land use and soil moisture studies.

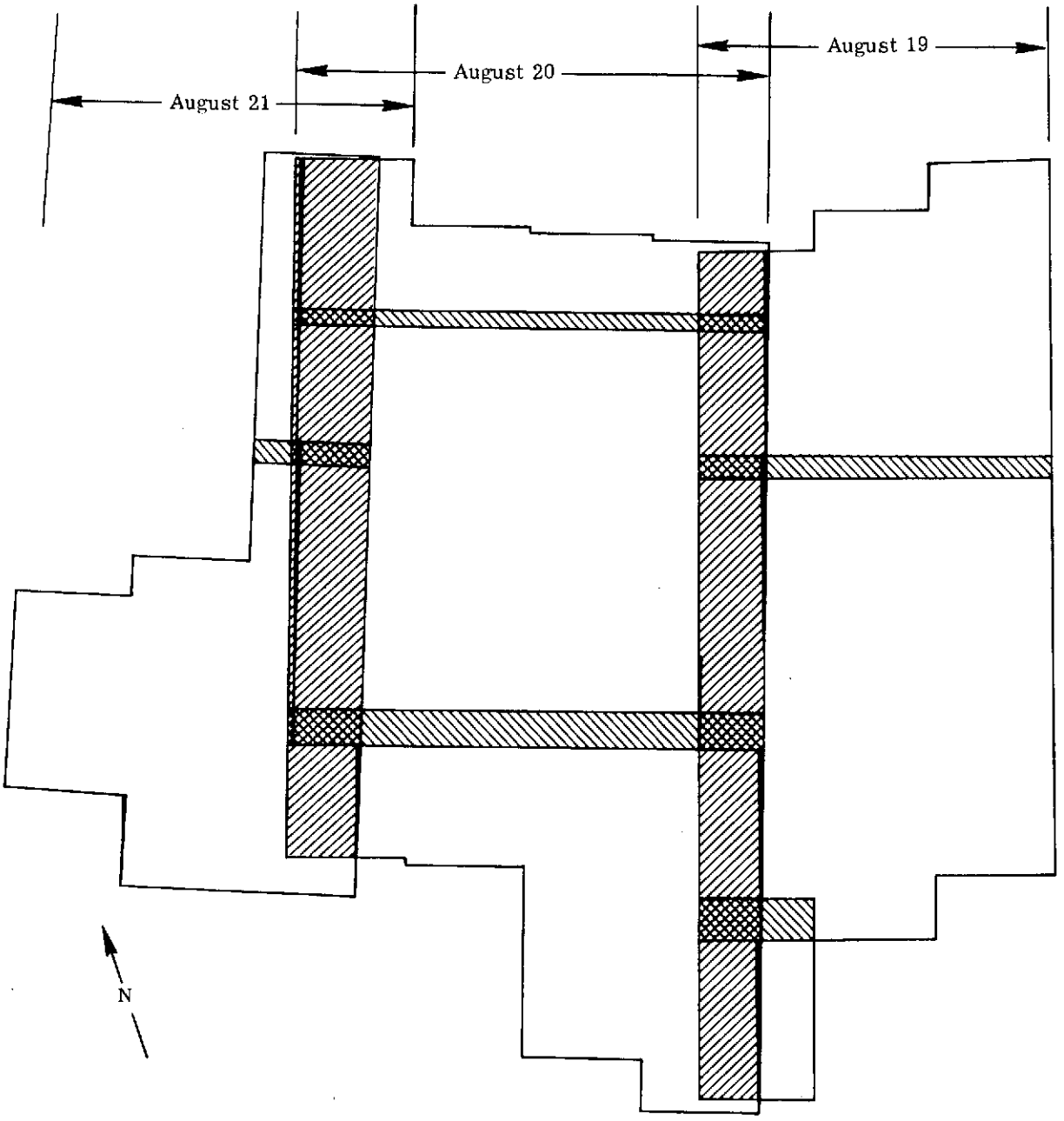

FIGURE 1. ERTS ANALOG TAPE COVERAGE OF LAKE ONTARIO BASIN

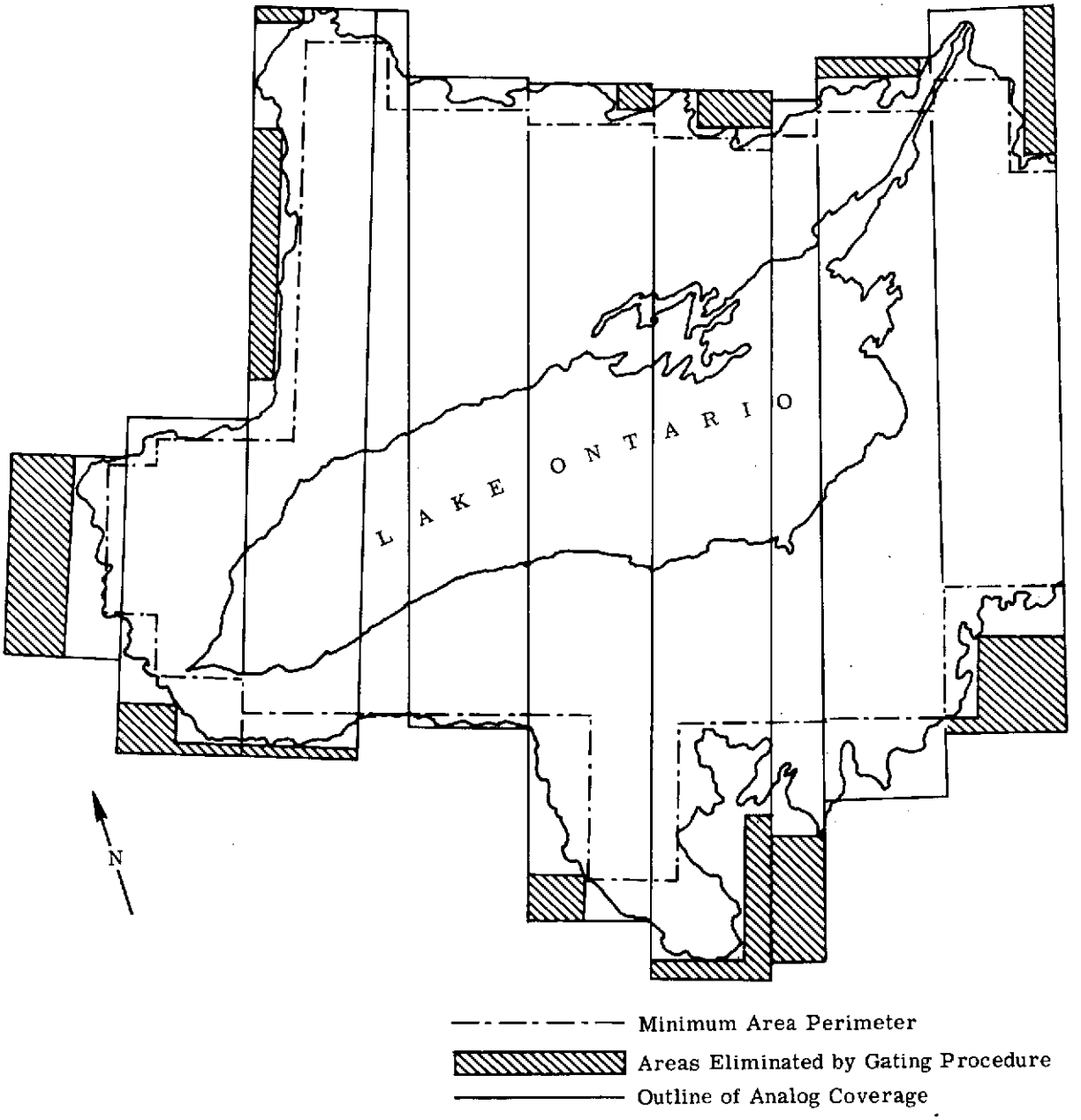

FIGURE 2. LAKE ONTARIO BASIN APPROXIMATION

ERIM
FORMERLY WILLOW RUN LABORATORIES, THE UNIVERSITY OF MICHIGAN

Sixth Type II Progress Report
Period: 1 July - 31 August 1973
W. A. Malila & R. F. Nalepka, MMC 136
Task VII, Image Enhancement and Advanced Information Extraction Techniques

INTRODUCTION

Experience has been gained at ERIM over the past decade in computer processing and extraction of information from airborne multispectral scanner (MSS) data and in modeling atmospheric effects in received radiance signals. The general objective of Task VII is to adapt techniques existing at ERIM for their application to ERTS-1 data, to assess the applicability of these techniques by applying them to selected ERTS-1 data, and to identify any additional problems that might be associated with such processing of satellite multispectral scanner data. Three areas are to be studied: (1) compensation for atmospheric effects in ERTS-1 data, (2) preprocessing for improved recognition performance, and (3) estimation of proportions of unresolved objects in individual resolution elements.

The intensive test site for this investigation is an agricultural area South-West of Lansing, Michigan, and the extensive test area also covers several other counties in South Central Michigan. A variety of agricultural crops and woodlots are in the intensive area. The primary crops are corn and wheat, with field beans, soybeans, and alfalfa also represented. The intensive test area is in an overlap region covered by ERTS-1 on two successive days of each 18-day cycle. Skies were clear on 25 August and ERTS data were collected. Simultaneous multi-altitude underflight coverage was obtained by the Michigan C-47 multispectral scanner aircraft, and ground-based measurements were made of spectral irradiance and sky radiance. RB-57 camera coverage of the region, obtained during June, was received in late September. A second RB-57 flight was made in mid-September, and its photography was received at the end of October. A second multispectral scanner aircraft mission was scheduled. Partial coverage was obtained in June, and the site for the remaining lines has been moved to the Willow Run Airport.

PROGRESS AND PLANS

The field instrumentation crew was on standby status for three ERTS cycles over the test site at Willow Run Airport for support of possible aircraft underflights in our study of atmospheric effects in ERTS-1 data. No flight was accomplished due to a combination of weather conditions and aircraft missions with higher priority. Attempts will be continued until a mission is carried out.

A rather extensive set of calibration measurements was made of the Bendix RPMI (Radiation Power Measuring Instrument) which has been made available for our use by Dr. Robert Rogers of the Bendix Aerospace Systems Division. This calibration information will be reduced and reported later.

The paper, "Correlation of ERTS MSS Data and Earth Coordinate Systems" by W. Malila, R. Hieber, and A. McCleer, whose abstract was included in the Type II Progress Report, 193300-16-P, July 1973, was completed.

ERIM
FORMERLY WILLOW RUN LABORATORIES, THE UNIVERSITY OF MICHIGAN

Sixth Type I Progress Report - 1 July 1973 - 31 August 1973
Task VIII - Water Quality Monitoring - 1400
C. T. Wezernak, UN 625, MMC 081

Work during the reporting period has been directed towards processing and analysis of data from the Lake Erie and New York Bight test sites. Several suitable frames have been received for W. Lake Erie together with high-gain data for the New York test site.

Additional processing and analysis of ERTS frame E-1247-15481 showing W. Lake Erie was performed. Analysis of frames E-1247-15481 and E-1265-15480 indicates a correlation between suspended solids (Total Non-filtrable Residue) and data integer level in band MSS 5. Black-white mosaics showing portions of Lake Erie have been prepared for the following scene dates:

(a) 12, 13, 14 April 1973 - entire lake,
(b) 7 June 1973 - W. Lake Erie,
(c) 25 June 1973 - W. Lake Erie.

The above imagery is being used to depict the movement of water masses and the introduction of suspended solids into the lake from major tributary sources. Ground-truth data in support of the analysis program is being compiled.

Initial digital processing of the high-gain data for the New York Bight (E-2194-15081, 13 May 1973) was performed. As anticipated, a three-fold increase in data integer levels in MSS 4 and 5 was realized. However, a line by line analysis of selected areas in the scene indicates the following:

1. A total integer level collapse every sixth line in MSS 4.
2. A periodic six line striping pattern in MSS 4 and 5.
3. Apparent loss of data as evidenced by periodic patterns of empty bins in the data.

As a consequence, the anticipated advantages of high-gain operation have not been realized in this particular data set. At the present time, the question remains unanswered as to what extent the anomalies described above are limited to this particular set. Initial analysis appears to indicate deficiencies in the process of producing high-gain computer compatible tapes. Additional analysis of the data set together with consultation with NASA is planned.

The feasibility of producing suitable high-gain CCT from ERTS-1 data is of great interest to this investigation. An increase in the dynamic range of the data set can be expected to contribute to an increased utility of ERTS-1 data in studies dealing with the aquatic environment.

Plans for the next bi-monthly period include digital processing of Lake Michigan data (9 June 1973), continued processing and analysis of Western Lake Erie (7 June 1973), and continued analysis of the New York high-gain data.

ERIM
FORMERLY WILLOW RUN LABORATORIES, THE UNIVERSITY OF MICHIGAN

Sixth Type I Progress Report - 1 July 1973 - 31 August 1973
Task IX - Oil Pollution Detection - 1389
R. Horvath, UN 606, MMC 079

Initial digital processing of MSS frames 1183-18175 and 1184-18234 to determine the detectability of a known oil slick in the Oakland (California) Inner Harbor has been completed. So far, no defineable anomaly associated with a possible slick signature has been found on the digital data.

There appears to be a number of deleterious effects contributing to this lack of detection: 1) the slick was 3 or 4 days old and quite tenuous at the time of ERTS data acquisition; 2) the Inner Harbor is quite narrow (3 to 6 pixels) and thus represents a poor background for detection of a radiometrically subtle anomaly; 3) the dynamic range of the data is compressed into a very few number of digital levels as a result of the very conservative MSS gain settings; and 4) raster noise associated with differences in gain and offset between the six detectors producing an MSS channel is of a magnitude comparable to that of the slick anomaly being sought. This latter problem is especially bad in MSS 6, where oil slick detection should otherwise be best. A computer program is now being implemented in order to correct all channels for this raster noise problem. Analysis will resume after this program becomes operational.

The accompanying table updates previously reported information regarding the relationship between major oil spill incidents and ERTS overflights. This tabulation is based upon official EPA spill reports through 21 June 1973. MSS imagery of the Monongahela River oil spill (overflight 5 June 1973) has been ordered from NDPF.

TABLE 1. COINCIDENCE OF MAJOR SPILLS AND ERTS OVERFLIGHTS

Location	Oil Type	Quantity	Report Date	Clean Date	ERTS Date	Comments
Salem, Mass.	#2 and #5 Fuel Oil	29,500 gal.	2 Oct. 72	after 4 Oct.	8 Oct. 72	Good Data Too late
Barataria Bay, Louisiana	Crude	336,000 gal.	9 Oct. 72	Dissipated before 17 Oct.72	18/19 Oct. 72	Overcast
San Antonio, Texas	Diesel Fuel	678,000 gal.	11 Oct. 72	≈ 17-18 Oct. 72	24 Oct. 72	Too late
San Juan City, New Mexico	Crude	100,000 gal.	12 Oct. 72	≈ 1 Nov. 72	16/17 Oct. 72	Overcast
Lake Barre, Louisiana	Crude	700 bbl.	22 Nov. 72	≈ 24 Nov. 72	23/24 Nov. 72	Overcast
Albemarle Snd, N. C.	Bunker, C	1000 gal.	28 Nov. 72	29 Nov. 72	3 Dec. 72	Good Data Too late
Gulf Coast Penzoil rig J, Storm II	Gas and oil (burning)	?	4 Dec. 72	6 Dec. 72	11 Dec. 72	Overcast Too late
Timbalier Bay, La. (well blowout)	Gas, Light	(minor ?)	6 Dec. 72	?	12 Dec. 72	Overcast
Jennings, La. (Bayou Nezpique)	Crude	3720 bbls.	14 Dec. 72	?	12/13 Dec. 72	Too early
Alameda, Ca. (Naval Air Station)	10% diesel 20% solvent 70% 20/40 lube	>1400 gal.	22 Dec. 72	23 Dec. 72	17 Dec. 72	Too early
Fenwick, Conn. (L. I. Sound)	#6 Fuel Oil	12,000 gal.	26 Dec. 72	30 Dec. 72	7 Jan. 73	Too late
Gulf Coast, La. (Pltfm A West Delta 79, Signal Oil Co.)	Crude	400,000 gal.	10 Jan. 73	11 Jan. 73 (Dissipated)	15/16 Jan. 73	Too late

TABLE 1. COINCIDENCE OF MAJOR SPILLS AND ERTS OVERFLIGHTS (CONT.)

Location	Oil Type	Quantity	Report Date	Clean Date	ERTS Date (SKYLAB Date)	Comments
Oakland, Ca.	Waste Oil	~120,000 gal.	19 Jan. 73	Contained 24 Jan. Completed 4 Feb.	22/23 Jan. 73	Tapes being processed
Vicksburg, Miss.	#2 Fuel Oil	4500 bbl.	31 Jan. 73.	3 Feb. 73 (Dissipated)	4 Feb. 73	Too late
Baton Rouge, La.	Crude	500,000 gal.	1 Mar. 73	Before 13 Mar. 73	12 Mar. 73	Too late
Bellingham, Wash.	?	est. 1000 gal. (7 sq. mi. slick)	2 Mar. 73	?	3 Mar. 73	Overcast
Cold Bay, Alaska	Diesel and Gasoline	235,000 gal.	9 Mar. 73 (start 8 Mar.)	18 Mar. 73	14/15 Mar. 73	Overcast
Houston, Texas	Oil and Diesel	420,000 gal.	12 Mar. 73 (start 9 Mar.)	19 Mar. 73	15 Mar. 73	Overcast
LaParguera, Puerto Rico	Crude	38,000 bbl.	19 Mar. 73	After 5 April 1973	29 Mar. 73	No Data Taken
Baton Rouge, La.	Slop Oil	40,000 gal.	28 Mar. 73	After 29 Mar. 73	30 Mar. 73	Overcast
Providence, R. I.	#6 Fuel Oil	50,000 gal.	12 Apr. 73	Before 20 Apr. 73	24 Apr. 73	Too late
Norfolk, Va.	Navy Distillate	30,000 gal.	27 Apr. 73	?	26 Apr. 73	Too early
Grand Isle, La.	Crude	240,000 gal.	11 May 73	15 May 73	22 May 73	Too late
Atchafalaya River Morgan City, La.	Crude	63,000 gal.	31 May 73	?	10 June 73 (11 June 73)	ERTS and SKYLAB both too late

TABLE 1. COINCIDENCE OF MAJOR SPILLS AND ERTS OVERFLIGHTS (Continued)

Location	Oil Type	Quantity	Report Date	Clean Date	ERTS Date (SKYLAB Date)	Comments
Monangahela River Duquesne, Pa.	#6 Fuel Oil	40,000 gal.	1 June 73	14 June 73	5 June	Images ordered
New York Harbor (M/V Exxon Brussels)	Crude	<80,000 gal.	2 June 73	Before 21 June 73	1 & 19 June 73	ERTS too early and too late
Santa Barbara Channel (Coal Oil Point)	Crude	Unknown seeping	5 June 73	?	13 June 73	Investigate ERTS
Oakland, Ca.	Bunker C	5,000 gal.	5 June 73	6 June 72	15/16 June 73 (2 June 73)	ERTS too late SKYLAB too early

ERIM
FORMERLY WILLOW RUN LABORATORIES, THE UNIVERSITY OF MICHIGAN

Sixth Type I Progress Report - 1 July - 31 August 1973
Task X - An ERTS Experiment for Mapping Iron Compounds - 1383
R. K. Vincent, UN422, MCC 075

General

The general objectives of this investigation are to develop a quantitative method for mapping lithologic units strongly associated with iron oxides, and to use this method to map iron oxides in the vicinity of the Wind River Range, Wyoming.

Progress During Period, 1 July - 31 August 1973

In this reporting period six ratio images and an automatic recognition map were made of an entire ERTS frame (E-1013-17294), a field trip was made to collect ground truth data, and temporal ratio maps were used to demonstrate that dark object subtraction and ratio normalization procedures described in the Second Type I report are correcting well for atmospheric and solar illumination effects. The automatic recognition map will be the main topic of the next bimonthly report, as it is currently being studied and compared with existing geologic maps and ground truth data from the field trip. It was constructed by making ratio inputs to a standard statistical decision method. Some stratigraphic mapping appears possible on a geochemical basis in the plains east of the Wind River Range, even though the grass cover is on the order of 40%. Besides the automatic recognition map (made with six ratios), an R_{54} (channel 5 divided by channel 4) ratio image delineates the hematitic Triassic red beds well, because the hematite is the brightest material in the scene in that image. This is in agreement with ratio codes calculated from laboratory data, which predict that hematite has a higher R_{54} ratio than 90% of the natural materials in the data bank. A list of materials and ratio codes is given in the recent Type II report for the period 1 January - 30 June 1973.

The field trip was successful, but only a small part (approximately 10%) of the processed ERTS frame could be observed owing to rugged terrain, unusually wet weather, and limited funds. Geologic maps will be used as ground truth for the rest of the frame. The bottom of the iron mine is composed mostly of magnetite ore, tailings, and some gangue rock of similar appearance. The Triassic red beds are strongly hematitic and are less vegetated than other members of the stratigraphic column near the Wind River Range. There is more grass cover than was expected on almost all targets; an overall estimate of grass cover (mostly brownish, even though it has been a wet year) on well exposed lithologic units in the region is 30-50%. It is encouraging that some geologic mapping can be done on a geochemical basis with so large an estimated percentage of grass cover. The only known natural iron ore outcroppings are not exposed in large enough areas to be identified on the recognition map. The typical naturally exposed iron ore in the area

was on the order of less than 100 meters in diameter, which would be less than one resolution element in ERTS data. The ground truth results will be used to interpret the recognition map and ratio images, which will be reported in the next two months.

A study to evaluate the effectiveness of the ratio method for suppressing atmospheric and solar illumination changes has been undertaken. The ratio method involves a subtraction of the radiance detected from the darkest object in a given scene (usually a quarter of an ERTS frame) from all other points in the scene for each ERTS MSS channel, a ratioing of the remaining radiances in two MSS channels, and a normalization of the ratio to a single known area (on the order of 5 to 10 spatial resolution elements) in the scene. These steps approximately eliminate the additive and multiplicative atmospheric and solar illumination terms, leaving a spectral ratio of target reflectances. The steps were explained in the second bimonthly report.

To assess the effectiveness of this procedure, a temporal ratio map was invented, which is produced in the following way. Spectral ratio maps (R_{75} for example) of two different ERTS passes are produced, with dark object subtraction and ratio normalization applied to correct for atmospheric and solar illumination effects. The two spectral ratio maps are merged such that they spatially coincide, and the spectral ratio map from one ERTS pass is divided by the spectral ratio map from the other ERTS pass to produce a temporal ratio map. If the empirical atmospheric and solar illumination corrections are effective, the temporal ratio should be at or near 1.0 for those objects on the ground which have not changed between ERTS passes. The area chosen for the temporal ratio map includes the iron mine near Atlantic City, Wyoming. The two ERTS passes were on 5 August 1972 (E-1013-17294) and 16 October 1972 (E-1085-17300). The 5 August frame had 0% cloud cover and was collected with sun elevation of 54.9° and sun azimuth of 130.2°, whereas the 16 October frame had 20% cloud cover (including some clouds in the scene used for the temporal ratio) and was collected with sun elevation of 34.0° and azimuth of 153.4°. Because of the differences in atmospheric state (evidenced by cloud cover) and sun position, these two frames offered a rigorous test of the empirical correction steps in the ratio method. The specific test site in the vicinity of the iron mine (which includes the ten resolution elements used for ratio normalization), was approximately 25% covered by cumulus clouds in the 16 October frame and was completely cloud free in the 5 August frame. The path radiance, as determined from dark object subtraction, was approximately the same for both frames, though the multiplicative atmosphere and solar illumination variables were significantly different in the two frames.

The procedure for testing the atmospheric and solar illumination invariance of the ratio method begins with an estimate of the number of elements (spatial resolution elements on the order of 100 meters in diameter) within the scene which had less than 50% vegetative cover in the 5 August frame and were uncovered by clouds in the 16 October frame. These elements, which will be called the ground invariant (GI) elements, represent the portion of the test area which is suspected not to have changed more than ±5% in spectral

reflectance between the two ERTS passes. The non-vegetated areas were determined from a thresholding of an R_{75} ratio of 1.20, which appeared to approximately delineate areas of less than 50% vegetation cover on the basis of ground photographs and observations made during the 21-27 July 1973 field trip to the test area. The vegetation is primarily a mixture of coniferous and deciduous trees, coarse grass, and sage. The cloud areas were delineated easily by ratioing ERTS MSS channel 7 for the 16 October frame to the same channel for the 5 August frame. [Note: Until the end of this discussion, the ratio of either spectral ratio or single channel radiance maps from two different ERTS passes will be called a temporal ratio map. At the end of this discussion and thereafter, temporal ratio map will refer only to the ratio for two ERTS passes of a spectral ratio that has been corrected by dark object subtraction and ratio normalization.] The resulting map of the GI elements is shown in Figure 1. The number of GI elements equaled 11,032 points out of a total of 25,125 points in the entire scene.

Next a temporal ratio map of ERTS MSS channel 7 was constructed, which is shown in Figure 2a, i.e., channel 7 radiance in the 16 October frame was divided by the channel 7 radiance in the 5 August frame. Figure 2b shows a temporal ratio map of ERTS MSS channel 5. In all of the temporal ratio maps to be discussed, the 16 October frame data are in the numerator, with 5 August data in the denominator. Also, in this and all other temporal ratio maps, lighter-toned areas represent small changes (small departures of the temporal ratio from 1.0) and darker-toned areas represent large changes; the key to interpreting the symbols in all of the temporal ratio maps is given in Table 1. There are only 361 elements in the scene which changed between ERTS passes by approximately ±5% or less (temporal ratio between 0.96 and 1.05) in the channel 7 temporal ratio, which represents only 3.27% of the GI elements (11,032). In the channel 5 temporal ratio map shown in Figure 2b, there were 1,122 elements (10.17% of the GI elements) in the scene which changed by ±5% or less. Because channel 7 changes more between ERTS passes than channel 5 and because the path radiance as determined from dark object subtraction is approximately the same for both passes, it is concluded that the change in solar illumination was greater than the change in atmosphere between 5 August and 16 October for this test site.

In Figure 3a is a temporal ratio map of a straight R_{75} spectral ratio, uncorrected by dark object subtraction and ratio normalization. The number of elements which changed by ±5% or less between ERTS passes in this case was 2,320 (21.02% of the GI elements). Thus, even an uncorrected R_{75} spectral ratio map is more invariant than single channel radiance maps to atmospheric and solar illumination variations. Shown in 3b is a temporal ratio map of an R_{75} spectral ratio, corrected by both the dark object subtraction and ratio normalization steps. For this case, the number of elements which changed by ±5% or less between ERTS passes was 11,032 (37.30% of the GI elements). Therefore, the corrective steps of the ratio method produce a spectral ratio map which is more invariant to atmospheric and solar illumination variations than either uncorrected spectral ratios or maps of single channel radiances.

As to the absolute effectiveness of the ratio method for suppressing atmospheric and illumination effects, the temporal ratio map procedure offers only an approximate answer. Table 2 shows the elements changing ±5% or less, ±10% or less, and ±15% or less between ERTS passes, expressed as a percentage of GI elements. This shows that the corrected R_{75} spectral ratio for this test site was invariant to atmospheric and illumination changes between 5 August and 16 October ERTS passes to within ±10% for 70% of the GI elements and to within ±15% for practically all of the GI elements (97%). These absolute numbers are only approximate because of three sources of error:

1. Some of the estimated GI elements could have changed more than ±5% during the ERTS passes by natural and unnatural causes.
2. The merging process is estimated to be accurate to within about two spatial resolution elements, which means that some points expected to be GI elements may show change only because of the merging process.
3. No attempt was made to discount points with small change that occurred in non-GI elements, though a comparison of Figures 1 and 3b shows that the vast majority of elements exhibiting small change in corrected R_{75} values are GI elements.

The first two sources of error make the results of Figure 2, Figure 3, and Table 2 appear worse than they actually are, whereas the third error source makes them appear better than actual fact. During the next reporting period, the third error will be corrected. These considerations and the above quantitative results indicate that the corrected R_{75} ratio map maybe invariant to atmospheric and illumination effects to within ±10% or better.

Plans for the Period, 1 September - 31 October 1973

The automatic recognition map will be compared with ground truth data and existing geologic maps of the test area during the next two months and a paper entitled, "Spectral Ratio Imaging Methods for Geological Remote Sensing from Aircraft and Satellites", which includes ratio images of ERTS data, will be presented on 31 October 1973 at the Management and Utilization of Remote Sensing Data Symposium of the American Society of Photogrammetry in Sioux Falls, South Dakota. Also, the temporal ratio assessment of how good the dark object subtraction and ratio normalization are performing will be refined and compared with normalized single channel gray maps, to determine whether the temporal ratio of spectral ratios would be best for ERTS investigators interested in change detection. The temporal ratio of spectral ratios was created to test the accuracy of empirical atmospheric and solar illumination variations, but it may become a spin-off useful to investigators in other disciplines.

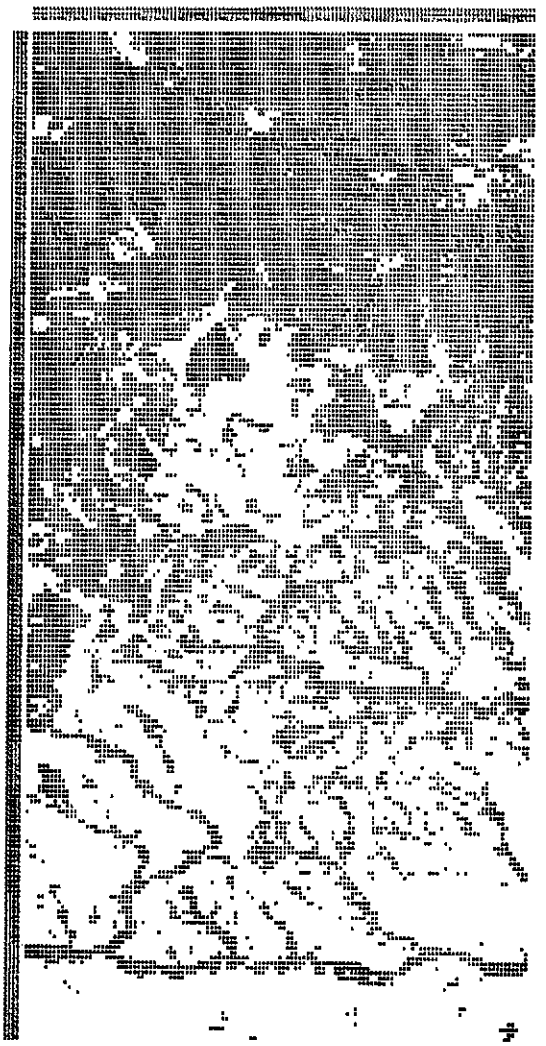

FIGURE 1. MAP OF ESTIMATED GROUND INVARIANT ELEMENTS BETWEEN 5 AUGUST AND 16 OCTOBER 1972 ERTS PASSES OVER TEST SITE NEAR ATLANTIC CITY, WYOMING. Dark symbols represent elements in the scene which have > 50% vegetation cover, or which are cloud-covered in the 16 October 1972 ERTS frame. Blank represents elements in the scene which are suspected to have changed less than 5% in spectral reflectance between ERTS passes.

TABLE 1.
KEY TO SYMBOLS FOR TEMPORAL RATIO MAPS IN FIGURES 2 AND 3

Temporal Ratio	Percent Change Between ERTS Passes	Symbols
≤ 0.80	≤ -200%	▓
0.81 to 0.85	-19% to -15%	¥
0.86 to 0.90	-14% to -10%	=
0.91 to 0.95	-9% to -5%	-
0.96 to 1.05	-4% to +5%	Blank
1.06 to 1.10	+6% to +10%	.
1.11 to 1.15	+11% to +15%	*
≥ 1.16	≥ +16%	θ

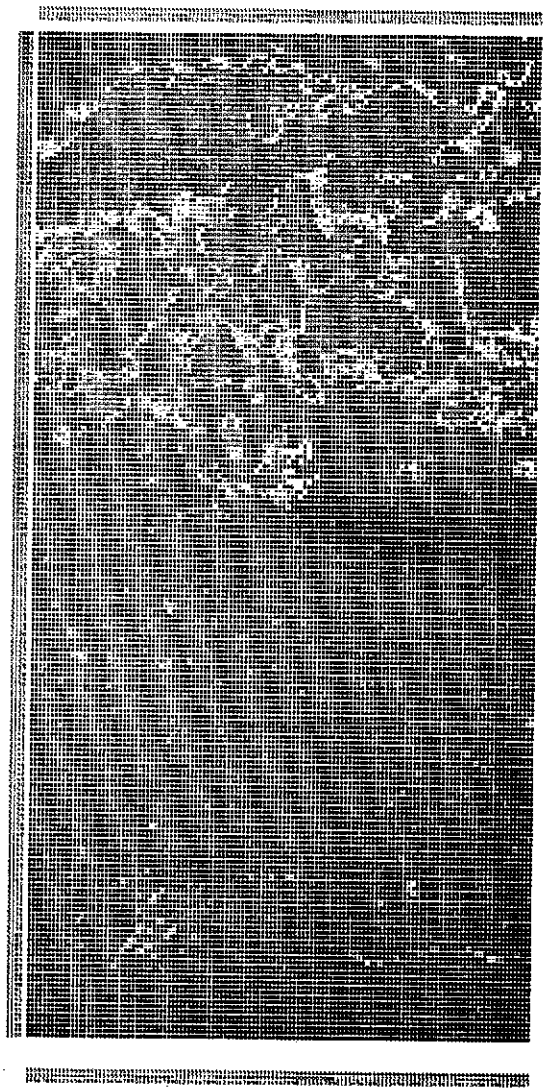

FIGURE 2a.

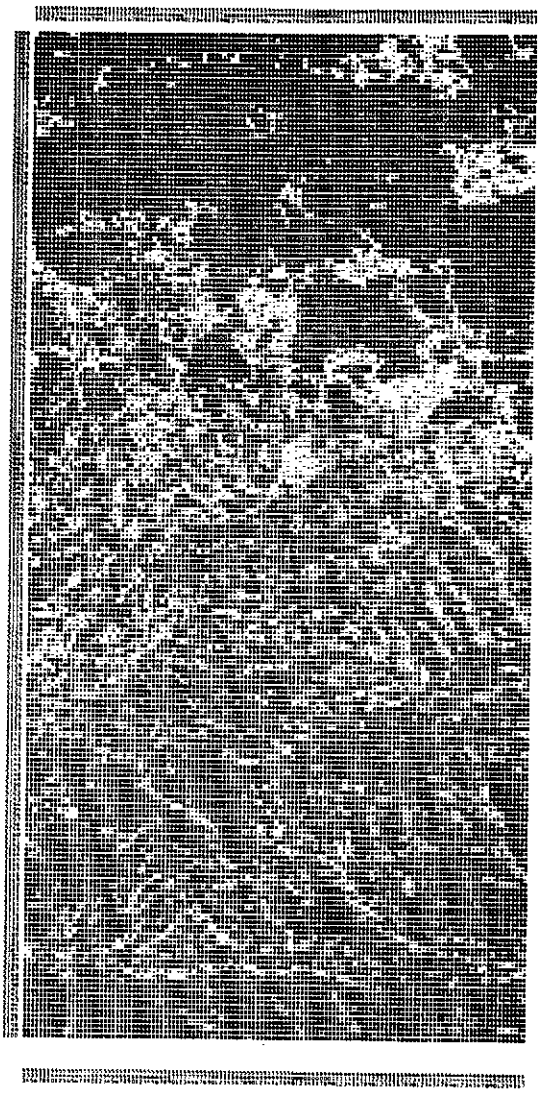

FIGURE 2b.

FIGURE 2. TEMPORAL RATIO MAPS OF ERTS MSS CHANNELS 7(2a) AND 5(2b) (16 OCTOBER 1972 FRAME DIVIDED BY 5 AUGUST 1972 FRAME) FOR TEST SITE NEAR ATLANTIC CITY, WYOMING. Lighter-toned symbols represent less change in the scene between ERTS passes (see Table 1 for key).

FIGURE 3a.

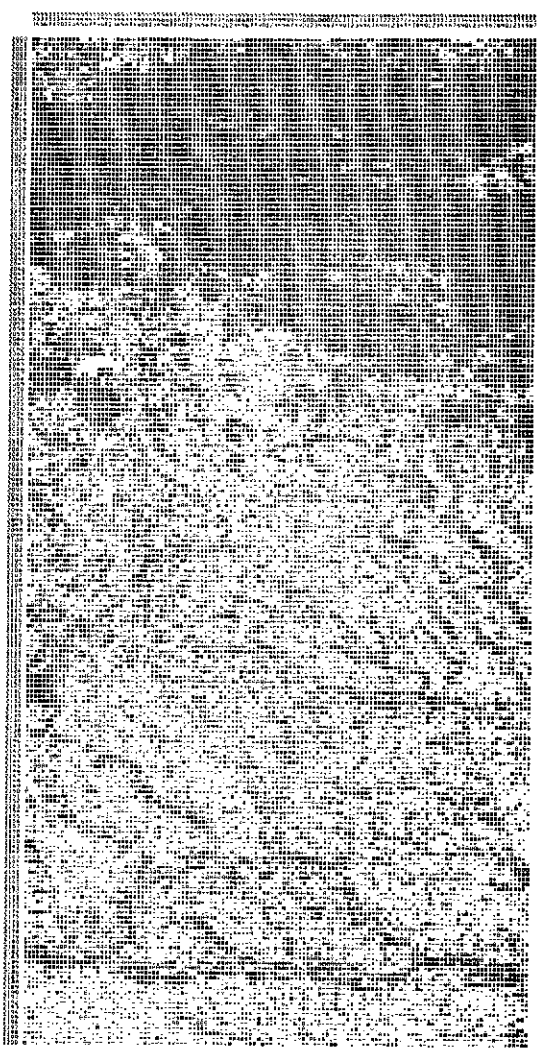

FIGURE 3b.

FIGURE 3. TEMPORAL RATIO MAPS OF UNCORRECTED R75 (3a) AND CORRECTED (3b) SPECTRAL RATIOS (16 OCTOBER 1972 FRAME DIVIDED BY 5 AUGUST 1972 FRAME) FOR TEST SITE NEAR ATLANTIC CITY, WYOMING. Lighter-toned symbols represent less change in the scene between ERTS passes (see Table 1 for key).

TABLE 2. Estimation of the absolute invariance of the R_{75} spectral ratio, corrected by dark object subtraction and ratio normalization, from a temporal ratio map of 16 October 72 and 5 August 72 ERTS passes over a test site near Atlantic City, Wyoming.

Percentage change in corrected R_{75} between ERTS passes	Number of Elements in the test area undergoing this percentage change	Percentage of estimated ground invariant elements in the scene (11,032 elements)
±5%	4,115	37.30%
±10%	7,745	70.20%
±15%	10,682	96.83%